2008-01-01

Assessment of Human Muscle Fatigue from Surface EMG Signals Recorded during Isometric Voluntary Contractions by using a Cosine Modulated Filter Bank

Cristhian Mauricio Potes
University of Texas at El Paso, cmpotes@miners.utep.edu

ASSESSMENT OF HUMAN MUSCLE FATIGUE FROM SURFACE EMG SIGNALS RECORDED DURING ISOMETRIC VOLUNTARY CONTRACTIONS BY USING A COSINE MODULATED FILTER BANK

CRISTHIAN MAURICIO POTES

Department of Electrical and Computer Engineering

APPROVED:

Ricardo F. von Borries, Ph.D, Chair

Nazeran-Esfahani Homayo, Ph.D.

Joseph Pierluissi, Ph.D.

Miguel Argaez, Ph.D.

Patricia D. Whiterspoon, Ph.D.
Dean of the Graduate School

To my

God, Future Wife, Parents, and Brothers

ASSESSMENT OF HUMAN MUSCLE FATIGUE FROM SURFACE EMG SIGNALS RECORDED DURING ISOMETRIC VOLUNTARY CONTRACTIONS BY USING A COSINE MODULATED FILTER BANK

by

CRISTHIAN MAURICIO POTES, E.C.E.

THESIS

Presented to the Faculty of the Graduate School of

The University of Texas at El Paso

in Partial Fulfillment

of the Requirements

for the Degree of

MASTER OF SCIENCE

Department of Electrical and Computer Engineering

December 2008

Acknowledgment

I would like to acknowledge the Air Force Research Laboratory, Human Effectiveness Directorate, for supporting this research (contract number FA8650-06-1-6748). In particular, I would like to acknowledge personnel in the Wright-Patterson Air Force Base, Drs. Zhiging Cheng and Ted Knox for helping with the electromyographic data set and providing important feedback along the project. A special thank you also goes to Mr. Nathan Wright, the Contract Monitor for this project. Mr. Wright's suggestions and constant supervision were essential for the successful conclusion of this project. This AFRL project opened new areas of research for students and faculty from the University of Texas at El Paso, UTEP.

I would like to profoundly thank my advisor Dr. Ricardo von Borries and my co-worker Cristiano Mendes Miosso for helping me with their knowledge and experience in the Digital Signal Processing field; this support was essential in the successful completion of this research project.

Finally, I would like to thank (1) Texas Instruments Foundation (TIF) for the given financial support during Fall 2007, Spring 2008, and Fall 2008 and (2) my professor Dr. Elaine Fredericksen for her valuable English Technical Writing course, which helped me to strongly improve my writing skills.

Abstract

Human muscle fatigue involves both a decrease in the frequency and increase in the amplitude of a surface electromyographic (EMG) signal. Muscle fatigue is also related to a decrease of the force impeding to reach the same initial level of the maximum voluntary contraction (MVC). To determine muscle fatigue indices, a method is proposed by decomposing a surface EMG signal into 32-subbands. This decomposition was attained by using a cosine modulated filter bank. The surface EMG signals analyzed during this research were recorded during isometric voluntary contractions. Both the instantaneous mean frequency (IMF) and the instantaneous amplitude (IA) are estimated from the 32-subbands of the filter bank and are used as indicators of muscle fatigue. For evaluating the IMF and the IA estimated from the filter bank, two other standard techniques, the spectrogram and the smoothed pseudo Wigner-Ville (SPWV) distribution, were also implemented.

A regression-free area ratio, introduced first by Merletti, was adopted to compute an EMG index from both estimates the IMF and IA. These indices were then classified – by using a joint analysis of frequency and amplitude (JASA) – into one of the four muscle activity regions: muscle increase force, muscle recovery, muscle decrease force, and muscle fatigue.

Surface EMG signals were recorded from 26 normal human subjects who exerted first 70% and then 100% of their MVC at intervals session of eight hours. It was found that EMG indices derived from the proposed filter bank are equivalent to those EMG indices derived from the spectrogram and the SPWV distribution. Furthermore, muscle fatigue indices derived from the filter bank indicated that they could be used as indices to determine human muscle fatigue. These results were confirmed by correlating the resulting muscle fatigue indices with perceived levels of discomfort reported by the subjects after performing an exertion of 70% MVC in hours two, four, and six.

Table of Contents

List of Figures

List of Tables

1
Theoretical Background

This chapter describes the theoretical background on human muscle fatigue. We divide this chapter into eight main sections: the first section briefly introduces the main purpose of this research, biomedical concepts, and some technical methods used in the assessment of muscle fatigue; the second section shows the relevance and impacts of this research in aerospace, military, ergonomics, and medical applications; the third section states two research questions; the fourth section describes the literature review; the fifth section defines some biological concepts involved in the muscle fatigue study; the sixth section explains physiological and surface electromyographic (EMG) changes manifested in muscle fatigue; and finally the seventh and eighth sections describe methods to estimate surface EMG variables when the signal is recorded during isometric and dynamic voluntary contractions.

1.1 Introduction

A method to quantify human muscle fatigue at the peripheral level, during isometric voluntary contractions, is introduced by decomposing surface EMG signals using a filter bank. Both the instantaneous mean frequency (IMF) and the instantaneous amplitude (IA) are estimated from the subbands of the filter bank and are used as indicators of myoelectric manifestations of human muscle fatigue.

Surface EMG refers to signals collected from the muscles by using electrodes which are placed in the skin's surface. Medical literature usually defines human muscle fatigue as a physical phenomenon where the muscle is unable to generate force leading to a sense of tiredness, lack of energy, and feeling of exhaustion [PvdMB06]

A majority of people have experienced muscle fatigue at some points in their lives; however, one could ask if all of them have experienced the same intensity. The answer is no. We may find cases where individuals report pain, while others report only discomfort. A problem arises when researchers want to compare muscle fatigue intensities among patients. In order to overcome this issue, muscle fatigue needs to be quantified. Muscle fatigue quantification from surface EMG signals requires the computation of indices based on physical variables that can be measured, such as force or torque, muscle fiber conduction velocity (MFCV), mean frequency, median frequency, and amplitude [MCO90], [KAFH07], [ZBvE08].

A reliable method to compute indices of muscle fatigue analyzing only surface EMG signals is still unclear. One of the reasons is especially because the information obtained from surface EMG signals is usually related to a large group of motor units [ZBvE08]. In addition, physical variables extracted from surface EMG signals are perturbed and masked by changes either in the central nervous system (CNS) or in the peripheral nervous system (PNS) [ZBvE08], [PvdMB06].

To reduce the number of factors affecting the surface EMG signal, this work focuses only on the assessment of muscle fatigue using surface EMG signals recorded during isometric voluntary contractions. These signals were provided by the Air Force Research Laboratory (AFRL) and were recorded from 26 healthy human subjects during prolonged wear of weighted flight helmets.

Muscle activity indices based on a regression-free area ratio [MCO90] are computed from the IMF and IA obtained from the spectrogram, smoothed pseudo Wigner-Ville distribution (SPWVD), and filter bank. These muscle activity indices are then classified using a joint analysis of spectrum and amplitude into four regions [LJL00a], [LJSL96]: muscle increase force, muscle recovery, muscle decrease force, and muscle fatigue. The resulting muscle fatigue indices are finally correlated to perceived levels of discomfort reported by the subjects.

1.2 Relevance of the Study of Human Muscle Fatigue

Assessment of human muscle fatigue has been an interesting research topic in the medical and engineering community because physiological changes associated to changes in the surface EMG

variables are still unclear. During muscle fatigue, surface EMG variables such as mean frequency, median frequency, and MFCV are related, although not exclusively, to pH decrease and lactic acid accumulation [Gan01], [ZBvE08]. For instance, lactic acid, a product involved in synthesizing adenosine triphosphate (ATP) without oxygen involvement, prevents pyruvic acid increases and aids pH decreases in the muscle cells [BA07]. Furthermore, lactic acid accumulation leads to a decrease in both MFCV and mean frequency [BPR$^+$91]. However, an opposite finding indicates that conduction velocity decreases in the absence of lactic acid, confirming that pH modification is not the only cause of muscle fatigue [ZBvE08].

Continuous quantification of muscle fatigue using non-invasive techniques has many practical applications in sports, rehabilitation medicine, ergonomics, aerospace jobs, and neuroengineering. For instance, in sports and rehabilitation medicine it is important to quantify muscle fatigue for monitoring muscle adaption to training or physical therapy. Quantification of muscle fatigue may also provide information on muscle behavior and muscle fiber type classification.

Muscle fatigue analysis has applications in occupational health and ergonomics. For instance, Luttman et al. analyzed muscle fatigue to evaluate surgeons performing urological endoscopic surgery. In this case, indices of muscle fatigue were used to justify surgeon's work place redesign [LJL00a].

Human muscle fatigue also has applications in external control of paralyzed muscles when using electrical stimulation. Knowing muscle fatigue intensity, electrical stimulation can be adjusted to avoid muscle injury.

Aerospace jobs demand, most of the time, physical and mental work for continuous long periods. For example, military pilots fly several hours wearing different weighted helmets, and NASA astronauts perform physically and mentally demanding intra-extra vehicular activities. These physically and mentally demanding activities lead to mental and muscle fatigue affecting the subjects' safety and performance [TKK$^+$05].

Changes in the weight and the head-helmet center of gravity of the new generation of military pilots' helmets may lead to neck fatigue and susceptibility to neck injury during aircraft ejections. As a result, continuous monitoring of muscle fatigue has been proposed as a potential tool to

evaluate military pilots' safety and performance during prolonged wear of weighted helmets.

Muscle fatigue also has applications in the diagnosis of neurological diseases. Disorders in the central nervous system comprise changes in the peripheral system and can be detected from surface EMG signals therefore. These peripheral system changes can be either a partial loss (paresis) or a total loss (paralysis) of muscle contraction [MP04].

1.3 Problem Statement

We define in this section the following two research questions:

1. Are the surface EMG variables (IMF and IA) estimated from the filter bank (proposed method) equivalent to those surface EMG variables estimated from the spectrogram and SPWV distribution?

2. Is there any relationship between muscle fatigue indices obtained from the filter bank and the perceived levels of discomfort reported by the subject?

1.4 Literature Review

This section shows several approaches proposed in the literature to assess human muscle fatigue. According to most researchers, the accuracy of muscle fatigue assessment depends on knowing under what physical conditions a surface EMG signal has been recorded. A surface EMG signal can be recorded during isometric or dynamic voluntary contractions [MP04].

Surface EMG variables such as frequency, amplitude, and MFCV have been employed to assess human muscle fatigue. However, this work focuses only on frequency and amplitude analysis. On one hand, the MNF and MDF have been proposed as spectral estimators. The root mean square (RMS), and the average rectified value (ARV), on the other hand, have been proposed as amplitude estimators [LJL00b], [Kon05], [FM00].

Spectral estimators depend on what technique is applied to estimate the power spectral density (PSD) of a surface EMG signal. If the surface EMG signal is recorded during constant-force iso-

metric voluntary contractions, Fourier-based transform is the most widely PSD estimator [MP04], [FM00]. On the contrary, if the signal is recorded during dynamic voluntary contractions, time-frequency analysis is the most used [MP04], [KYA98], [KGa01].

In order to describe several approaches to assess and quantify muscle fatigue, we divide this section into three main bodies: (1) frequency and amplitude estimation during isometric voluntary contractions, (2) frequency and amplitude estimation during dynamic voluntary contraction, and (3) computation of muscle fatigue indices based on frequency and amplitude changes.

1.4.1 Isometric Voluntary Contractions

Most of the literature regarding human muscle fatigue reports frequency decreases and amplitude increases when the surface EMG signal is recorded during constant-force isometric voluntary contractions [KAFH07], [SK00]. Frequency decreases are mainly attributed to MFCV decreases, and amplitude increases are probably attributed to motor unit recruitment [KAFH07], [LJSL96], [Kon05], [LJL00a], [ZASF07] [FM00].

Surface EMG is considered a wide sense stationary (WSS) random process during short time intervals (epochs); therefore, its PSD can be estimated using classical estimators: periodogram and time-varying autoregressive models [KAFH07], [LJSL96], [LJL00a], [ZASF07], [FM00]. Note that during this type of contractions, the surface EMG signal is considered WSS inside time intervals lasting from 1 s to 2 s. [1]

MNF and MDF estimation from the periodogram are explained in [KAFH07], [LJSL96], [LJL00a], [ZASF07], [FM00]: (1) the surface EMG signal is divided into equal epochs of duration 500 ms or 1 s; (2) the PSD of each epoch is then estimated by applying the absolute value squared of its Fourier transform; and finally (3) the MNF and MDF are computed from each estimated PSD. Some authors suggest epochs overlapping of 50% to reduce the variance of the estimator [LJSL96], while others state that epochs overlapping increase the computational time without improving spectral variables estimation [FM00].

PSD of a surface EMG signal can also be estimated using time-varying autoregressive models

[1] In this work, we define s for seconds.

(TVAR). Selection of the TVAR model order is not critical; a model order of 10 seems to be appropriate for epochs of 125 ms, 250 ms, 500 ms, and 1 s [FM00]. TVAR can be used to estimate the MNF and MDF of a surface EMG signal and to monitor muscle fatigue development during isometric voluntary contractions [zFK06], [zA05].

A few studies report that the accuracy of PSD estimation depends on several factors such as PSD estimation technique and size and shape of the time window. Moreover, PSD estimation requires the surface EMG signal be stationary within short time windows; such stationarity is not valid for contractions greater than 50% MVC [XW06]. To overcome these difficulties, Georgakis et al. propose to estimate the instantaneous frequency of a surface EMG by computing the first derivative of the phase of its Hilbert transform [GSG03].

Several authors point out that this method is useful to estimate the instantaneous frequency of monocomponent signals, e.g., signals with only one frequency component, or at least a narrow bandwidth. However, Huang et al. state that in the case of multicomponent signals, such as surface EMG signals, one would obtain at some points negative frequencies and frequencies outside the bandwidth of the signal [XW06], [HAO06]. Consequently, this method is not suggested to estimate the instantaneous frequencies of surface EMG signals.

An alternative solution to this issue, based on the Hilbert-Huang transform, is proposed in [XW06]. The HHT consists of decomposing a signal into a set of intrinsic mode functions, in such a way that they may then be Hilbert transformed. Xie et al. [XW06] conclude that the HHT is the best choice to analyze changes in the surface EMG frequency.

In summary, there are several techniques reported in the muscle fatigue literature to estimate the frequency of a surface EMG signal. However, these techniques depend on PSD estimation and signal stationarities. Additionally, most of the articles report frequency decreases and amplitude increases as manifestations of muscle fatigue when the surface EMG signal is recorded during constant-force isometric voluntary contractions.

1.4.2 Dynamic Voluntary Contractions

The study of muscle fatigue is more complex for surface EMG signals recorded during dynamic voluntary contractions than for surface EMG signals recorded during isometric voluntary contractions. This is because the surface EMG signal becomes non-stationary during dynamic voluntary contractions; therefore, simple Fourier-based transforms are no longer valid to estimate the surface EMG frequency.

Muscle fatigue literature also reports frequency decreases and amplitude increases during dynamic voluntary contractions [PB97]. However, one should take care when interpreting muscle fatigue associated with frequency decreases. Frequency decreases might not necessarily be related to physiological muscle fatigue changes: pH decreases and lactic acid increases [LKP77].

Time-frequency distributions have been recently adopted in the assessment of muscle fatigue during dynamic voluntary contractions. The advantage of a time-frequency distribution, excepted the spectrogram, is that the signal's frequency content can be extracted without considering segments of the signal to be stationary. Note that the spectrogram, the same as the periodogram, can be applied to assess muscle fatigue only when the signal has slow non-stationary components; i.e., signals recorded during constant-force isometric voluntary contractions.

Recent studies report several approaches to estimating a time-frequency distribution. These approaches are classified as linear and bilinear time-frequency distributions. The linear time frequency distributions are the spectrogram and wavelets, and the bilinear time-frequency distributions are mainly the Wigner-Ville (WV), Choi-Williams (CW), and smoothed pseudo Wigner-Ville (SPWV).

A comparison of the WV, SPWV, and CW is attained in [BRKL01], [BGK96], [DDMM95]. Bonato et al. claim that the WV distribution is an efficient tool to analyze monocomponent signals; however, WV's performance to analyze multicomponent signals is negatively affected by cross terms. Cross terms, undesirable in the analysis of muscle fatigue, are artifacts perturbing the frequency and amplitude estimation of a surface EMG signal. In order to avoid these cross terms, the WV distribution can be modified by convolving it with a smoothing function (kernel). The SPWV and CW are two time-frequency distributions based on the WV distribution that employ

different kernels to reduce cross terms. Bonato et al. [BGK96] report that (1) the SPWV has the disadvantage of destroying signal components in the cross terms rejection, and (2) the CWD seems to be very effective in cross terms rejection and in retaining most of the time-frequency distribution properties.

Wavelet and Wavelet packets (WP) have been recently introduced in the analysis of muscle fatigue [KPB03], [KG04], [KYA98], [RA97], [Tsc00], [KGa01], [SK00], [SPBJ00]. For instance, muscle fatigue is approached in [KPB03] by determining the wavelet decomposition of the signal, using wavelets Sym4 or Sym5, and eight or nine iteration levels in the decomposition. In addition, some authors have proposed to estimate the MNF of a surface EMG signal by using WP. By comparing (1) MNF curves derived from WP with (2) MNF curves obtained from the spectrogram, it is inferred that both (1) and (2) exhibit qualitatively similar shapes and trends [RA97]. WP does not show cross terms as does the WV distribution and has the advantage, compared to the traditional time-frequency distributions, of being the only one that allows frequency resolution for different frequency regions [KYA98], [Tsc00].

A comparison of the CW and the continuous wavelet transform (CWT) is performed in [KGa01] and [SK00]. These studies report that the CW is the most suitable time-frequency distribution to represent non-stationary biological signals; however, its use requires careful selection of the kernel parameters. Kernel parameters selection should be adapted to each specific signal. Karlsson et al. claim that the CWT is very reliable for the analysis of signals recorded during static and dynamic contractions without requiring any smoothing function; frequency estimation based on the CWT is less noisy than CW. Moreover, Karlsson et al. report amplitude increases as the force increases, and frequency decreases as the force decreases. The main drawback of the CWT is that it is computationally expensive and requires large storage requirements. Discrete wavelet transform (DWT) has been proposed to overcome this issue [KPB03], [KG04], [KYA98], [RA97], [Tsc00].

1.4.3 Indices of Muscle Fatigue

Quantification of muscle fatigue can be represented by the time course increases or decreases of a surface EMG variable. Muscle fiber conduction velocity, spectral variables (MNF, MDF), and

amplitude variables (RMS, ARV) show a linear or curvilinear behavior, depending on the muscle contraction level and the experimental condition. For instance, low-level muscle contractions lead to linear decreases of MFCV, MNF and MDF, whereas high-level muscle contractions lead to curvilinear decreases of the same variables [LKP77], [MCO90].

Changes over time in the surface EMG variables (decreases or increases) have been fitted to regression models (e.g., linear or exponential models); regression parameters such as the slope have been used as a muscle fatigue index [RM04], [MCO90].

By using a linear regression model, slopes can be computed to measure the decrease or increase rate of the estimated frequency and amplitude [KAFH07], [LJSL96], [XW06], [LJL00a], [SPBJ00], [ZASF07], [FM00]. A joint analysis of the spectrum and amplitude (JASA) has been proposed to classify frequency and amplitude slopes into four stages: (1) increase force when both the frequency and the amplitude slopes increase, (2) recovery when the frequency slopes increase and the amplitude slopes decrease, (3) decrease force when both the frequency and the amplitude slopes decrease, or (4) fatigue when the frequency slopes decrease and the amplitude slopes increase [LJSL96], [LJL00a]. A simultaneous frequency and amplitude analysis of the surface EMG allows to discriminate fatigue-induced and force-related surface EMG changes [LJL00a].

Muscle fatigue indices based on regression parameters depend on the choice regression model, which varies according to the experimental condition. For instance, frequency slopes obtained using a linear regression model could not be compared with frequency slopes obtained using an exponential regression model [MCO90].

As a result, Merletti et al. [MCO90] propose a new fatigue index based on a regression-free area ratio. This fatigue index can be computed to any surface EMG variable (MFCV, MNF, MDF, ARV, RMS), varies between 0 and 1 for decreasing patterns, and is negative for increasing patterns. According to Merletti [MCO90], a fatigue vector whose components are the regression-free muscle fatigue indices obtained from each surface EMG variable may be used to classify muscle contraction. Additionally, a closer measure of the muscle fatigue intensity can be obtained from this area-ratio index compared to other muscle fatigue indices used in previous studies.

Although JASA and a Merletti's index help to quantify muscle fatigue, their relationship with

physiological muscle fatigue changes, such as pH increases and lactic acid increases, demands additional investigation.

1.5 The Concept of Human Muscle Fatigue

Every human being may have felt muscle fatigue when performing a long high-intensity activity, but without being able to measure the strength of the fatigue. Muscle fatigue is not a physical variable, and its intensity depends on each subject's physiology. To know the muscle fatigue intensity without using invasive techniques, researchers have proposed to estimate muscle fatigue indices from physical variables such as force and firing rate or from surface EMG variables such as amplitude, frequency, and MFCV [MP04].

Human muscle fatigue starts during the onset of a muscle contraction and develops progressively until the muscle cannot generate force. In addition, the maximal force or maximum voluntary contraction (MVC) decreases once the muscle starts contracting.

Human muscle fatigue may have peripheral or central causes [Gan01]. Neuromuscular junction (peripheral nervous system or PNS) changes may produce muscle fatigue characterized by a reduction in the force-generation capacity. Muscle contraction stimulus starts in the brain; therefore, muscle fatigue may also be caused if the central nervous system (CNS) cannot stimulate the neuromuscular junction. This brain's inability to stimulate the neuromuscular junction is known as central fatigue and may be caused by lack of concentration or alertness or loss of motivation [Sch05].

One of the characteristics of human muscle fatigue is the muscle's inability to sustain the same initial MVC force. In voluntary contractions, force depends on the motor unit recruitment and the firing rate [zA05]. The greater the motor unit recruitment and the firing rate, the greater the force [MP04].

Increases in muscular force are also related to amplitude and frequency increases in the surface EMG signal. Frequency increases are attributed to action potential increases, which are also attributed to firing rate increases [LJL00a].

Motor unit recruitment is the continuous recruitment of motor units, and firing rate is the rate in which a single motor unit fires the muscle fiber [Gan01], [MP04]. Both motor unit recruitment and firing rate are factors involved in the produced force intensity.

A single motor neuron and its stimulated muscle fibers compose a motor unit. A motor neuron controls muscle contraction and carries impulses from the brain and spinal cord to the muscles. The α-motor neurons are a certain type of motor neurons localized in the brainstem and the spinal cord. The α-motoneurons localized in the brainstem innervate the head and neck muscles, while the α-motoneurons localized in the spinal cord innervate the remaining muscles of the body [MP04].

Some studies have identified three types of motor units based on physiological properties and fatigability: (1) motor units type I or S (slow-twitch) characterized for being the most resistant to fatigue, (2) motor units type IIa or FR (fast twitch) characterized for being fatigue-resistant, and (3) motor units type IIb or FF (fast twitch) characterized for being vulnerable to fatigue [ZASF07].

Researchers have studied human muscle fatigue during isometric and dynamic voluntary contractions. During constant-force isometric voluntary contractions, subjects, at static position, sustain constant force at different MVC levels for a certain time period. The term isometric comes from static muscle contraction; i.e., the joint angle and muscle length do not change during the exercise. In contrast, during dynamic voluntary contractions, subjects sustain dynamic force; the joint angle and muscle length change during this contraction. Examples of dynamic voluntary contractions are walking, bicycling, swimming, etc.

1.6 Myoelectric Manifestations of Human Muscle Fatigue

Human muscle fatigue involves physiological changes affecting force production; these changes are mainly lactic acid accumulation, pH decreases, and metabolic byproducts increases (free phosphate). Depending on the type of sustained voluntary contraction, these physiological manifestations may indirectly lead to changes in the surface EMG amplitude and frequency. The physiological and surface EMG changes manifested during muscle fatigue are explained in detail below.

1.6.1 Physiological Changes

Clinical neurophysiology studies indicate that decrements in the force during muscle fatigue are mainly attributed to changes in the action potential, as well as in the extracellular and intracellular ions [ZBvE08]. For instance, peripheral nervous system changes, such as lactic acid accumulation and pH decreases, affect the membrane excitability during muscle fatigue.

Muscles rely on adenosin triphosphate (ATP) production as their energy source. ATP can be created either with oxygen (aerobic glycolysis) or without oxygen (anaerobic glycolysis). Aerobic glycolysis produces 6 or 8 moles of ATP and 2 moles of pyruvate; the complete oxidation of the 2 moles of pyruvate, through the TCA cycle, yields to 30 moles of ATP. Therefore, a complete oxidation of one mole of glucose yields a total of 36 or 38 moles of ATP. In contrast, anaerobic glycolysis produces pyruvate and only 2 moles of ATP; the enzyme lactate dehydrogenase (LDH) converts the pyruvate into lactic acid [Sch98]. It is important to remark that anaerobic glycolysis generates lactic acid; lactic acid prevents the increase of pyruvic acid, contributes to the decrease of the pH in the muscle cells, and is considered the major cause of muscle fatigue [AHJDR86].

Muscle fatigue is mainly attributed to a lack of energy to fuel muscle contraction. During intense muscle activity, the cardiovascular system can not deliver enough oxygen and blood to the muscle cells; therefore, there is a decrement in the energy to fuel the muscle cells. As a result, the muscle cells have to compensate for this energy depletion by synthesising more ATP through anaerobic glycolysis. This ATP synthesis results in lactic acid accumulation leading to muscle fatigue.

1.6.2 Surface EMG Changes

Measured variables extracted from surface EMG signals have been widely studied to quantify muscle fatigue. These surface EMG variables are mainly amplitude, frequency, and MFCV, and they are very sensitive to neuromuscular physiological phenomena. For instance, Stulen et al. proved that changes in the frequency content and conduction velocity during isometric constant force contractions can be used as indicators of muscle fatigue and may be related to motor unit

type [FdL82].

The precise estimation of surface EMG variables depends on anatomical, physical and methodological factors. Some of these factors are (1) fiber length, (2) number of motor units, (3) variation of the electrodes location with respect to the active muscle, (4) inter-electrode distance, and (4) surface EMG variable estimators [MP04].

Typical characteristics of muscle fatigue during submaximal isometric voluntary contractions are (1) amplitude increases, (2) frequency decreases, and (3) MFCV decreases. Amplitude increases are attributed to the motor unit recruitment, whereas frequency and MFCV decreases are attributed to lactic acid accumulation [ZBvE08]. In addition, Luttman et al. report that amplitude increases are caused by force increases or fatigue [LJL00a]. Sparto et al. studied back muscle fatigue during isometric voluntary contractions at 70% MVC [SPBJ00]. In this paper, the authors report that amplitude increases in the low frequency signal can be related to an increase in motor unit firing, whereas amplitude decreases in the high frequency signal can be related to a reduction in the action potential conduction velocity. However, these results have not always been consistent when assessing muscle fatigue from surface EMG signals recorded during dynamic and sustained maximal voluntary contractions. For instance, it has been shown that amplitude decreases and frequency increases when assessing muscle fatigue during sustained maximal voluntary contractions [KT79],[Kon05].

1.7 Isometric Voluntary Contractions

During isometric voluntary contractions the surface EMG signal may be considered wide-sense stationary (WSS) for time intervals (epochs) lasting 0.5 to 2 s [MP04]. The mean frequency (MNF) and median frequency (MDF) have been widely employed as spectral variables of the surface EMG signal; the fast Fourier transform (FFT) has been extensively used to estimate these spectral variables for WSS signals. In addition, the amplitude of the surface EMG signal has been estimated by using RMS and ARV.

1.7.1 Methods to Estimate Surface EMG Variables

Spectral Estimators

The periodogram has been the Fourier-based spectral estimator to estimate the MNF and the MDF of a WSS zero mean discrete time random process. By definition, the periodogram is a power spectral density (PSD) estimator of a finite signal, which is obtained by windowing one random process realization $x(n)$. Let $x_w(n) = w(n)x(n)$ be the windowed random process, and $w(n)$ be a M-point window function; the rectangular window has been frequently used in muscle fatigue analysis. Then the periodogram is defined as

$$S_{x,M}(f) = \frac{1}{M}\left|\sum_{n=0}^{M-1} x_w(n)e^{-j2\pi fn}\right|^2, \tag{1.1}$$

where f is the discrete frequency variable defined as $f = (0, 1, 2, \ldots, M-1)\frac{1}{M}$.

The expected value of the periodogram when M tends to infinity is equal to the true spectrum; i.e., the estimator (periodogram) is asymptotically unbiased. However, the periodogram is not a minimum variance estimator due to its variance does not tend to zero as M approaches to infinity. Consequently, the average of multiple periodograms obtained from overlapping or nonoverlapping random process segments has been proposed to reduce the variance estimation.

The MNF of $x_w(n)$ can be estimated from 1.1 by computing the first order moment of the periodogram:

$$\hat{f} = \frac{\sum_{i=0}^{M-1} f_i S_{x,M}(f_i)}{\sum_{i=0}^{M-1} S_{x,M}(f_i)}. \tag{1.2}$$

The MDF is the frequency that divides the PSD in two equal power parts. The MDF of $x_w(n)$ can also be estimated from 1.1:

$$\sum_{i=0}^{k} S_{x,M}(f_i) = \frac{1}{2}\sum_{i=0}^{M-1} S_{x,M}(f_i), \tag{1.3}$$

where f_k is the MDF.

Both spectral variables, the MNF and MDF, have been extensively proposed in muscle fatigue assessment to measure PSD changes of the surface EMG signal. However, it is still unclear which spectral variable is the best to detect these changes. For instance, some authors claim that the MDF is less sensitive to noise; others claim that the MNF is more stable and sensitive to PSD changes [LJSL96].

Amplitude Estimators

The RMS and ARV have been proposed in the muscle fatigue literature as amplitude estimators of the surface EMG signal. The RMS, also known as the quadratic mean, is defined as the square root of the mean of the squares of a windowed random process $x_w(n)$. The ARV is defined as the absolute value mean (rectification) of a windowed random process $x_w(n)$. Both equations to compute the RMS and ARV are shown below:

$$RMS_{x,M} = \sqrt{\frac{1}{M}\sum_{n=0}^{M-1} x_w(n)^2}, \tag{1.4}$$

$$ARV_{x,M} = \frac{1}{M}\sum_{n=0}^{M-1} |x_w(n)|\,. \tag{1.5}$$

1.8 Dynamic Voluntary Contractions

The study of muscle fatigue during dynamic voluntary contractions is more complex than during isometric voluntary contractions. This is because the muscle changes its size and position with respect to the electrodes during dynamic voluntary contractions . This phenomenon may introduce nonstationarities in the surface EMG signal; hence, the FFT is no longer used to estimate surface EMG spectral variables [MP04]. To estimate surface EMG frequency changes during isometric voluntary contractions, it is assumed that the motor unit is stable. Stability of the motor unit in this context is defined by Merletti et al. [MP04] as, ”Motor unit of the active pool are not inactivated

or replaced with fresh ones during the contraction." This stability does not occur during dynamic voluntary contractions; instead there is a constant derecruitment of motor units. Therefore, a decrease in the frequency might not be a sufficient condition to assert muscle fatigue during dynamic contractions. [MP04].

Time-frequency distributions can overcome Fourier transform difficulties in analyzing non-stationary signals. A time-frequency distribution aims to provide information about how the surface EMG energy is distributed over time and frequency. Additionally, the instantaneous mean frequency (IMF) and instantaneous amplitude (IA) can be computed from time-frequency distributions as explained below.

1.8.1 Methods to Estimate Surface EMG Variables

In this section, we briefly describe different methods to estimate the IMF and IA of a surface EMG signal collected during dynamic voluntary contractions. We start describing linear time-frequency distributions such as the short time Fourier transform (STFT) and wavelets. Then we describe bilinear time-frequency distributions namely Wigner-Ville, Choi-Williams, and the Smoothed Pseudo Wigner-Ville. Finally, we explain some time-frequency properties and how to compute the IMF and the IA from any time-frequency distribution.

Linear Time-Frequency Distributions

a. **Short Time Fourier Transform (STFT)**

The STFT can be computed first by sliding a window along a random process and taking the Fourier transform of each segment. Let $x_w(n) = x(n)w(n-d)$ be a segment of the random process, and $w(n-d)$ be a M-point sliding window with delay parameter d. Then the STFT of $x(n)$ can be computed as

$$STFT(n,f) = \sum_{n=0}^{M-1} x(n)w(n-d)e^{-j2\pi fn}. \tag{1.6}$$

The spectrogram, squared magnitude of the STFT, has been widely used in muscle fatigue analysis for signals recorded during isometric voluntary contractions. However, its use has been poor for the analysis of signals recorded during dynamic voluntary contractions. This is because the surface EMG frequency estimation assumes the signal is stationary inside the analysis window [XW06]. This stationary assumption, as explained in section 1.7, is only valid for surface EMG signals recorded during isometric voluntary contractions. Another drawback of the STFT is called time-frequency localization trade-off. This means that a small window leads to high time resolution but poor frequency resolution, whereas a large window leads to high frequency resolution but poor time resolution.

b. **Wavelets**

To overcome issues such as time-frequency localization trade-off and stationary signal assumption, wavelet transform introduces the idea of using short windows for high frequencies and long windows for low frequencies. The wavelet transform does not defined a fixed time-window as does the STFT.

The continuous wavelet transform of an input signal $x(t)$ is defined as

$$CWT_{\psi x}(a,\tau) = \int x(t)\psi^*_{a,\tau}(t)dt, \tag{1.7}$$

where $a > 0$ is the scale parameter, τ is the time shifting parameter, $\psi_{a,\tau}(t)$ is a scale version of the mother wavelet $\psi(t)$. and $*$ denotes the complex conjugate of a function.

$$\psi_{a,\tau}(t) = \frac{1}{\sqrt{a}}\psi\left(\frac{t-\tau}{a}\right). \tag{1.8}$$

A discrete wavelet transform (DWT) can be implemented by passing a discrete signal $x(n)$ through a series of low pass and high pass filters. Discrete WP, a variation of the DWT, was recently introduced by Karlsson et al. [SK00] to analyze surface EMG signals. Karlsson et al. report that the mean square error of the spectral variables estimated using discrete WP

is less than the mean square error of those spectral variables estimated using Fourier-based transform.

Bilinear Time-Frequency Distributions

a. **Wigner-Ville (WV) distribution**

The WV distribution of a discrete signal $x(n)$ is defined as

$$W(n,f) = 2\sum_{-\infty}^{\infty} x(n+k)x^*(n-k)e^{-4j\pi fk}. \tag{1.9}$$

In multicomponent signal analysis, this distribution is negatively affected by cross terms, which limits its use in muscle fatigue studies. These cross terms introduce errors in the estimation of the IMF.

To overcome this problem, bidimensional smoothing functions (kernels) have been proposed to reduce cross terms. Additionally, desirable properties of the distribution can be accomplished by constraining the kernel function. The Choi-Williams distribution and the smoothed pseudo Wigner-Ville distribution define two different kernels to make the WVD suitable in the muscle fatigue analysis. The kernel of these two distributions are explained next.

b. **Choi-Williams (CW) distribution**

The kernel for the CWD is defined as

$$\phi(\nu,\tau) = e^{-\frac{(\pi\nu\tau)^2}{2\sigma^2}}. \tag{1.10}$$

Note that the WVD is obtained for this distribution when $\sigma \rightarrow +\infty$. Likewise, the cross terms are almost zero when $\sigma \rightarrow 0$. The distribution efficiency strongly depends on the choice of σ, which has to be adapted according to the surface EMG signal nature. A good selection of σ is in the range from 0.1 to 10 [SK00]

c. **Smoothed Pseudo Wigner-Ville (SPWV) distribution**

As shown in section 1.8.1, the spectrogram is dependent on a short-time window yielding to a time-frequency localization trade-off. In order to make the smoothing function more

independent in both time and frequency, the SPWV distribution introduces a separable kernel function defined as

$$\phi(\nu, \tau) = g(\tau)H(\nu),$$

where $H(\nu)$ is a frequency smoothing window, and $g(\tau)$ is a time smoothing window. Both $H(0)$ and $g(0)$ are forced to be 1. Cross terms reduction depends on the choice of the frequency and time smoothing functions.

Time-Frequency Distribution Properties

Time-frequency analysis is an important tool in the development of muscle fatigue indices since the frequency and the amplitude of the surface EMG signal can be estimated from a time-frequency distribution. Evaluation of the spectrogram, wavelets, WV distribution, CW distribution, and SPWV distribution are based on the following desired properties.

a. **Time and Frequency Marginals**

The time and frequency marginals of a joint time-frequency distribution $P(n, f)$ of a discrete signal $x(n)$ are respectively given by

$$P(n) = \sum_{f=-\infty}^{\infty} P(n, f) = |x(n)|^2 \tag{1.11}$$

and

$$P(f) = \sum_{n=-\infty}^{\infty} P(n, f) = |X(f)|^2 = \left| \sum_{n=-\infty}^{\infty} x(n) e^{-j2\pi fn} \right|^2, \tag{1.12}$$

where $X(f)$ is the discrete-time Fourier transform of the discrete signal $x(n)$, $P(n)$ is the time marginal, and $P(f)$ is the frequency marginal. If the time-frequency distribution satisfies the time and frequency marginals, then according to 1.11 and 1.12 the time and frequency

marginals must be, respectively, the instantaneous energy and the energy density spectrum of the analyzed signal.

b. **Time and Frequency Finite Support**

If a discrete signal $x(n)$ is zero inside the time interval $[n_1, n_2]$, then a time-frequency distribution satisfying $P(n, f) = 0$ for $n \in [n_1, n_2]$ is expected. Similarly, if the spectrum of a signal $x(n)$ is zero inside the frequency interval $[f_1, f_2]$, then a time-frequency distribution satisfying $P(n, f) = 0$ for $f \in [f_1, f_2]$ is expected [Coh95], [PS03].

c. **Time and Frequency Localization**

The time localization of a signal $x(n)$ at time n_0 is given by

$$x(n) = \delta(n - n_0) \Rightarrow P(n, f) = \delta(n - n_0, f),$$

and the frequency localization at frequency f_0 is given by

$$X(f) = \delta(f - f_0) \Rightarrow P(n, f) = \delta(n, f - f_0)$$

[PS03].

d. **Positivity**

Wigner demonstrated that any bilinear distribution that satisfies the time and frequency marginals cannot always be positive; it must have regions of negative values for any signal. However, Cohen showed that there exist time-frequency distributions that are not bilinear but are positive and satisfy the marginals. One of the advantages of having a time-frequency distribution that is positive and satisfies the marginals is that the distribution also satisfies the time and frequency finite support [Coh95].

e. **Suppression of Cross Terms**

Cross terms are artifacts or interference terms that are undesirable in the muscle fatigue analysis because they negatively affect the IMF estimation. These cross terms are introduced

by the bilinearity of some distributions such as the Wigner-Ville distribution. For instance, consider a discrete signal $x(n)$ be expressed as the sum of two parts $x_1(n) + x_2(n)$. The WV distribution of $x(n)$ is then given by

$$WV(n,f) = WV_{11}(n,f) + WVD_{22}(n,f) + WV_{12}(n,f) + WV_{21}(n,f),$$

where $WV_{12}(n,f)$ and $WV_{21}(n,f)$ are the cross-WV distribution. Therefore, the WV distribution of the sum of two signals is not the sum of the WV distribution of each signal. It also adds cross terms interfering with the analysis of the distribution.

f. **Window Independence**

The aim of introducing a time-frequency window is to reduce cross terms and to better localize the quick changes of the surface EMG signal. However, these windows destroy desirable properties of a distribution such as the time and frequency marginals and time and frequency support. Furthermore, the choice of the time-frequency window size play an important role in the assumption of the stationarity of the surface EMG signal, as well as in a time-frequency localization trade-off. A time-frequency localization trade-off implies that a good localization in time leads to a poor localization in frequency and vice-versa.

g. **Energy Conservation**

The total energy of an ideal joint time-frequency distribution should be the total energy of the signal $x(n)$ [Coh95]

$$E = \sum_{n=-\infty}^{\infty} \sum_{f=-\infty}^{\infty} P(n,f) = \sum_{n=-\infty}^{\infty} |x(n)|^2 = \sum_{f=-\infty}^{\infty} |X(f)|^2.$$

IMF and IA Estimation from a Time-Frequency Distribution

The IMF and IA can be estimated from a time-frequency distribution. The IMF $\hat{f}(n)$ is estimated as the first order moment of the frequency distribution for a given time

$$\hat{f}(n) = \frac{\sum_{n=-\infty}^{\infty} fP(n,f)}{\sum_{n=-\infty}^{\infty} P(n,f)}, \tag{1.13}$$

and the IA $A(n)$ is estimated as the square root of the time marginal

$$A(n) = \sqrt{P(n)} = \sqrt{\sum_{f=-\infty}^{\infty} P(n,f)} = |x(n)|. \tag{1.14}$$

2
Materials and Method

This chapter describes the materials and method used in this project to assess muscle fatigue. First, we present subjects with their anthropometry measurements and neck muscles to be studied. Second, we describe how the surface EMG signals were recorded from the AFRL. Finally, we explain how it is estimated the IMF and IA of the signal, and how it is compute the muscle fatigue indices from the estimated IMF and IA.

2.1 Materials

Muscle fatigue was evaluated from surface EMG signals recorded from 26 normal human subjects: 11 females and 15 males. The females had an average age of 23 years, average weight of 146 pounds, and average height of 163 cm. The males had an average age of 27 years, average weight of 184 pounds, and average height of 177 cm. Surface EMG signals were acquired at a sampling frequency of 1024 Hz from six neck muscles: left and right trapezius, left and right splenius capitis, and left and right sternocleidomastoid (See Fig. 2.1).

A Delsys Bagnoli-8 EMG system with DE-2.1 standard differential EMG electrodes was used for the collection of the myoelectric data. Prior to entrance into the study, basic anthropometry measurements (age, weight, height) were collected from each subject to ensure that they fulfilled the requirements of the study.

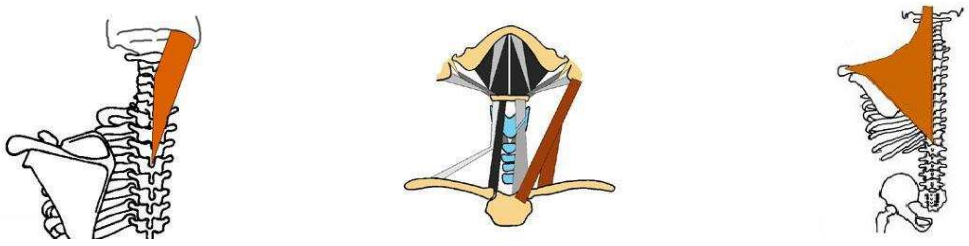

(a) (b) (c)

Figure 2.1 Neck muscles involved in the analysis of muscle fatigue. (a) Muscle – Splenius capitis; Action – Extends and rotates cervical spine. (b) Muscle – Sterno; Action – Flexes and laterally rotates cervical spine. Extends neck when neck is already partially extended; (c) Muscle – Trapezius. Action – Stabilizes, elevates, retracts, and rotates scapula (source – AFRL).

2.2 Study Design

For this research, 3480 surface EMG recorded signals provided by the Air Force Research Laboratory are analyzed for the muscle fatigue evaluation. The objective of this analysis is to present indices to measure neck muscle fatigue during prolonged wear of weighted flight helmets. These indices are useful in the development of guidelines to guarantee good performance and safety to pilots. In this study, each subject was exposed to five sessions of eight hours with a minimum waiting period of 48 hours between them. In each session the subject wore a different weighted flight helmet as shown in Fig. 2.3, and Table 2.1. They also performed a 100% maximum voluntary contraction (MVC) before and after the eight-hour session, and a 70% MVC at the end of every hour (first hour to seventh hour). A 70% MVC was sustained for a maximum time period of three minutes. The subject could stop the muscle contraction before the three minutes if the subject could not sustain the exertion any longer.

Figure 2.2 shows a dynamometer used to monitor the strength given by the subject's neck muscle during the 70% and 100% MVC exertion. During this strength monitoring, surface EMG data were recorded to measure the change in muscular activity and to analyze muscle fatigue. During each session of eight hours, the subjects completed a comfort survey before the initial 100% MVC, after hours two, four, seven, and after the final 100% MVC. After collection of the

data, the surface EMG signal of each subject was normalized to 100% MVC as suggested by Merletti [RM04].

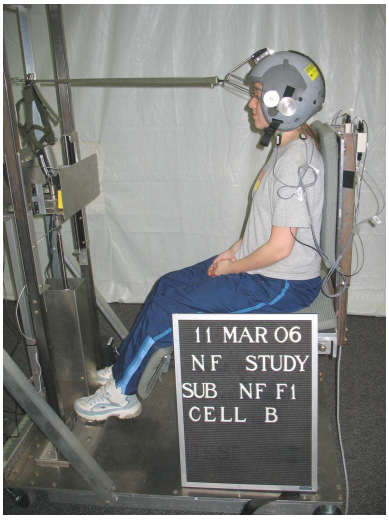

Figure 2.2 Dynamometer. The Neck Strength Monitoring Device is used to monitor 100% MVC and 70% MVC. The helmet is attached to a cable that is connected to a stationary load cell. The subject will pull rearward using only neck muscles. Source: AFRL

Table 2.1 Helmet configurations (Air Force Research Laboratory).

Cell	Weight (Lb)	Helmet Center of Gravity (CG)
A	3.0	Baseline
B	4.5	Near head
C	4.5	Forward head
D	6.0	Near head
E	6.0	Forward head

2.3 Method

This section explains our proposed method to quantify human muscle fatigue. First, we introduce the idea of using filter banks to analyze surface EMG signals. Second, we describe how to estimate the IMF and IA from a filter bank decomposition. Finally, we present an approach to compute muscle fatigue indices based on a regression-free area ratio [MCO90].

Figure 2.3 Helmet. The center of gravity of the helmet can be set to provide different configurations. Source: AFRL

2.3.1 Filter Bank

In muscle fatigue analysis, it is very important to know how the frequency content of a signal changes over time. A filter bank allows researchers to decompose a signal into its frequency components. A filter bank looks like a prism where the input signal (in this case white light) is separated into a spectrum of colors.

Analysis is the process when the input signal is decomposed into its different frequency components (subbands). Synthesis is the process when the signal is reconstructed back from its subband components. In our muscle fatigue assessment, we only do the analysis part using a bank of 32 filters.

The 32 subbands of the surface EMG analysis are obtained by filtering the recorded surface EMG signal $x(n)$ with a cosine modulated filter bank of $F = 32$ channels (see the cosine filter bank in Fig. 2.5). Each component of the 32 subbands are then squared, forming a time-frequency representation of the surface EMG signal as shown in Fig. 2.4. Each subband component is given by

$$y_i(n) = \left(\sum_{k=-\infty}^{\infty} x(k) h_i(n-k) \right)^2, \tag{2.1}$$

for $i = 0, 1, 2, \ldots, F-1$. Note that each subband $y_i(n)$ has length $N = L + M - 1$, where L is the filter length; and M is the signal length. A time-subband representation $Y(f, n)$ of the signal

$x(n)$ can be expressed in matrix form as

$$\mathbf{Y(f,n)} = \begin{bmatrix} y_{0,0} & y_{0,1} & y_{0,2} & \cdots & y_{0,N-1} \\ y_{1,0} & y_{1,1} & y_{1,2} & \cdots & y_{1,N-1} \\ y_{2,0} & y_{2,1} & y_{2,2} & \cdots & y_{2,N-1} \\ \vdots & \vdots & \vdots & \vdots & \vdots \\ y_{F-1,0} & y_{F-1,1} & y_{F-1,2} & \cdots & y_{F-1,N-1} \end{bmatrix}_{F \times N} \tag{2.2}$$

The frequency ranges **f** for each subband are defined as

$$\mathbf{f} = \frac{\text{Fs}}{2F} \begin{bmatrix} 0 & 1 & 2 & \ldots & F-1 \end{bmatrix}^T \tag{2.3}$$

where Fs is the sampling frequency. Since we use a Fs $= 1024$ Hz and a total of subbands $F = 32$, our resulting frequency ranges are then

$$\mathbf{f} = \begin{bmatrix} 0 & 16 & 32 & 48 & \ldots & 496 \end{bmatrix}^T. \tag{2.4}$$

2.3.2 Instantaneous Mean Frequency Estimation (IMF)

We propose to estimate the IMF of a surface EMG signal by using the same definition that Cohen shows in [Coh95]. Cohen proposes to estimate the IMF by computing the first order moment of the frequency distribution at a certain point in time. The only difference here is that the IMF is estimated from our proposed time-subband representation instead of being estimated from any of the Cohen's time-frequency representations.

The instantaneous mean frequencies in each time instant are defined in a vector **y** as

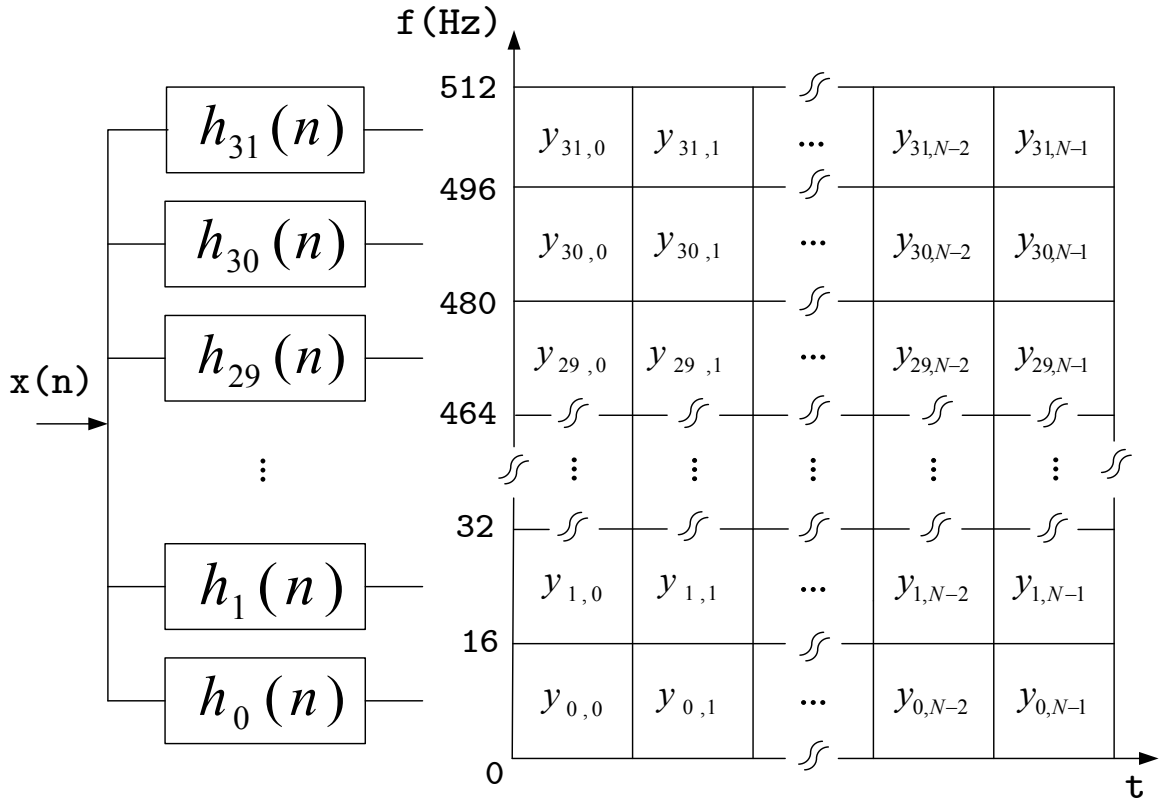

Figure 2.4 Filter bank analysis. The signal $x(n)$ is filtered by a cosine modulated filter bank of 32 channels. The resulting coefficients of each subband are then squared and organized in a time-frequency matrix representation. There are 32 rows representing the subbands and N columns representing the discrete time. The total of columns N is given by $L + M - 1$, where L is the filter length, and M is the signal length.

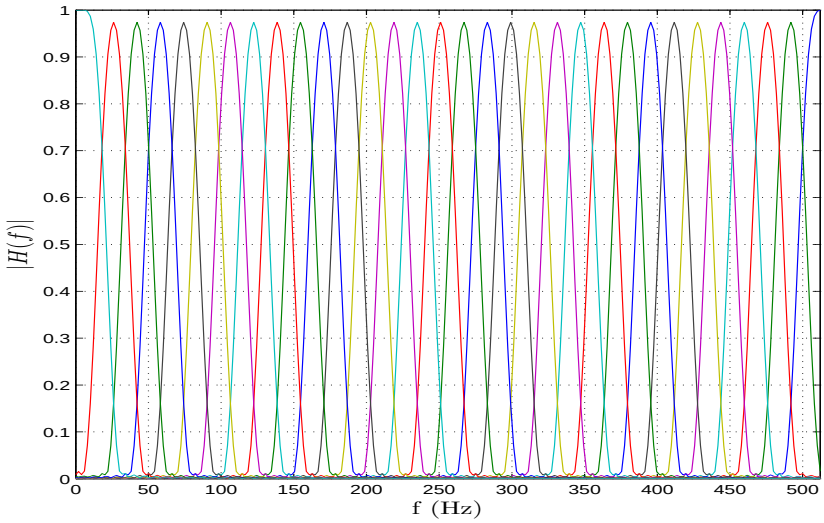

Figure 2.5 Cosine modulated filter bank of 32 channels.

$$\mathbf{y} = \mathbf{Y}^T\mathbf{f} = \begin{bmatrix} y_{0,0} & y_{1,0} & y_{2,0} & \cdots & y_{F-1,0} \\ y_{0,1} & y_{1,1} & y_{2,1} & \cdots & y_{F-1,1} \\ y_{0,2} & y_{1,2} & y_{2,2} & \cdots & y_{F-1,2} \\ \vdots & \vdots & \vdots & \vdots & \vdots \\ y_{0,N-1} & y_{1,N-1} & y_{2,N-1} & \cdots & y_{F-1,N-1} \end{bmatrix}_{N\times F} \begin{bmatrix} f_0 \\ f_1 \\ f_2 \\ \vdots \\ f_{L-1} \end{bmatrix}_{F\times 1} \tag{2.5}$$

All the IMF are normalized by dividing all the components of the resulting vector **y** with all the components of a vector **v**. Each component v_j of the vector **v** is defined as

$$v_j = \sum_{i=0}^{F-1} y_{i,j}, \tag{2.6}$$

for $j = 0, 1, 2, \ldots, N-1$.

Finally, the resulting normalized IMF components $\hat{f}_i$ are obtained from 2.5 and 2.6 as

$$\hat{f}_i = \frac{y_i}{v_i}, \tag{2.7}$$

for $i = 0, 1, 2, \ldots, N-1$.

In this work, we propose to average the resulting IMF in time intervals of 250 ms or 500 ms

$$\hat{f}_l = \frac{1}{l} \sum_{i=0}^{l-1} \hat{f}_i, \tag{2.8}$$

where l is the existing number of samples inside a time interval. For instance, the total number of samples for a time interval of 250 ms using a Fs $= 1024$ Hz are 256.

2.3.3 Instantaneous Amplitude Estimation

To estimate the IA from the time subband representation, the following sequential stages are proposed: (1) define a rectangular window for each subband with a length that is inversely proportional to the central frequency of the subband; (2) find in each subband the maximum coefficient inside the window; and, finally, (3) add all the corresponding maximum values to obtain an estimate of the IA. The estimate of the IA for the next point in time is computed by shifting the rectangular window one sample to the right, and then steps (1) to (3) are repeated until the IA is estimated along all the signal.

2.3.4 Fatigue Indices

Previous studies have proposed to compute muscle fatigue indices based on the rate of change of measured surface EMG variables. For instance, decreases or increases rate of the frequency and amplitude can be estimated by computing the frequency and amplitude slopes. However, computation of these indices depend on how well a regression model fits the data.

In this work, we apply Merletti's idea [MCO90] to compute muscle fatigue indices from the IMF and IA estimation. In this paper, Merletti et al. propose a regression-free muscle fatigue index, which depends only on the estimated surface EMG variable.

A regression-free index F is defined as the ratio of the area A and a reference area R as shown in Fig. 2.6. The reference area can be computed as $R = A + B = y_r t_c$, where y_r is a reference value, and t_c is the duration of the contraction. In this work, we choose the first sample of the

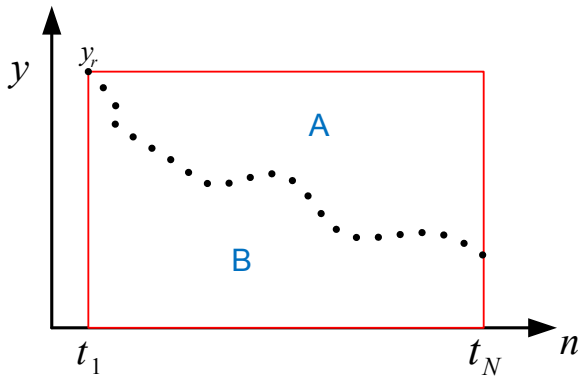

Figure 2.6 Definition of the regression-free index. The reference value y_r is defined as $y_r = y_1$)

.

surface EMG variable to be analyzed as y_r.

There is a general expression to compute the regression-free index F when the surface EMG variable is equally spaced in time:

$$F = 1 - \frac{1}{2(N-1)y_r} \sum_{i=1}^{N-1} (y_i + y_{i+1}), \tag{2.9}$$

where N is the total number of samples of the surface EMG variable. Note that if N is replaced by K, for $2 \leq K \leq N$, then the regression-free index F becomes a function of time. The next point F_{k+1} can be computed without reusing Equation. 2.9 as

$$F_{k+1} = \left(1 - \frac{1}{k}\right) F_k + \frac{1}{k} \left(1 - \frac{y_{k+1} + y_k}{2y_r}\right). \tag{2.10}$$

The regression-free index F shows a fatigue curve with respect to time in the following way: (1) if the surface EMG variable shows a decrease pattern then $0 \leq F \leq 1$, and (2) if the surface EMG variable shows an increase pattern then $F \leq 0$. There is no fatigue when $F = 0$, whereas there is rapid fatigue when $F \approx 1$.

In brief, this index, proposed by Merletti, is regression-free and provides a quantitative approach of muscle fatigue.

2.3.5 Joint Analysis of Spectrum and Amplitude

A joint analysis of the spectrum and amplitude (JASA) of a surface EMG signal was first introduced by Luttman et al. in [LJSL96]. To do this analysis, we need to fit a linear regression model to a surface EMG variable (e.g., the frequency and amplitude estimates). The slope, given by this linear regression model, can describe the decrease or increase rate of the frequency or amplitude in order to track the ongoing muscle fatigue.

Muscle fatigue indices based on these slopes assume that the time course of the surface EMG variable always show a linear behavior, but what happen with those surface EMG variables that show a different pattern (e.g., a curvilinear behavior)? To overcome this issue, we propose in this project to combine Merletti's and Lutman's ideas in order to quantify muscle fatigue.

After estimating the IMF and IA using the filter bank, we compute muscle fatigue indices for each surface EMG variable, F_{IMF} and F_{IA}, using Merletti's method described in section 2.3.4. We name a muscle fatigue index derived from the IMF surface EMG variable as F_{IMF}, and a muscle fatigue index derived from the IA surface EMG variable as F_{IA}. The F_{IMF} and F_{IA} are computed for epochs of 30 s, thus providing a muscle fatigue index curve over time. We name $\hat{F}_{IMF}$ and $\hat{F}_{IA}$ to the quantities computed by integrating the muscle fatigue index curve F_{IMF} and F_{IA} over the three-minutes recording. Note that for both $\hat{F}_{IMF}$ and $\hat{F}_{IA}$, a negative quantity corresponds to increases surface EMG variables, while a positive quantity corresponds to decreases surface EMG variables. Finally the $\hat{F}_{IMF}$ and $\hat{F}_{IA}$ are classified using JASA analysis into four muscle activity regions (see Fig. 2.7): (1) muscle increase force when both the $\hat{F}_{IMF}$ and $\hat{F}_{IA}$ are negative; (2) muscle recovery when the $\hat{F}_{IMF}$ is negative and the $\hat{F}_{IA}$ is positive; (3) muscle decrease force when both the $\hat{F}_{IMF}$ and $\hat{F}_{IA}$ are positive; and (4) muscle fatigue when the $\hat{F}_{IMF}$ is positive and $\hat{F}_{IA}$ is negative.

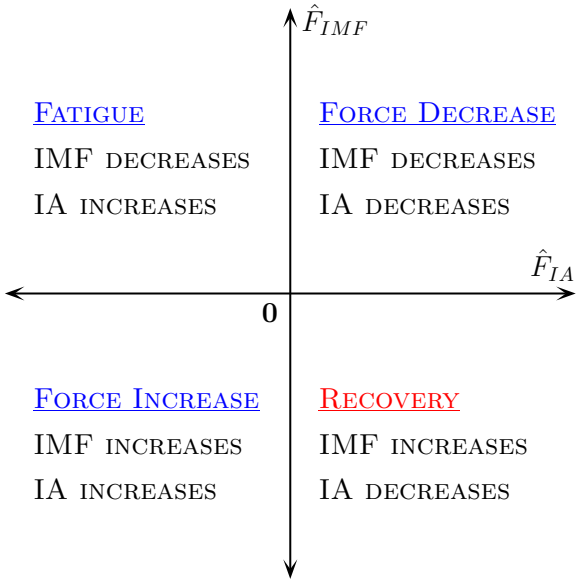

Figure 2.7 Joint Analysis of Frequency and Amplitude (JASA). Classification of the EMG indices into four muscle activity regions: (1) muscle increase force when both the $\hat{F}_{IMF}$ and $\hat{F}_{IA}$ are negative; (2) muscle recovery when the $\hat{F}_{IMF}$ is negative and the $\hat{F}_{IA}$ is positive; (3) muscle decrease force when both the $\hat{F}_{IMF}$ and $\hat{F}_{IA}$ are positive; and (4) muscle fatigue when the $\hat{F}_{IMF}$ is positive and $\hat{F}_{IA}$ is negative.

3
Results

This chapter describes the experimental results obtained when surface EMG signals, provided by the AFRL, were analyzed using the filter bank decomposition. This chapter is divided into two main bodies: section 3.1 compares the IMF and IA muscle fatigue indices estimated using the filter bank decomposition, with the IMF and IA muscle fatigue indices estimated using the spectrogram and SPWV distribution; section 3.2 shows muscle fatigue indices obtained from the spectrogram, SPWV, and filter bank decomposition in the muscle fatigue analysis of a female subject.

The comparison described in section 3.1 is based on the computation of Pearson's correlation coefficient and the relative quadratic difference. The muscle fatigue indices described in section 3.2 are correlated with the perceived levels of discomfort reported by the subject. These discomfort levels were also provided by the AFRL.

3.1 Comparison of the IMF and IA

We computed muscle fatigue indices from the IMF and IA surface EMG variables. The F_{IMF} and F_{IA} were estimated using the spectrogram, SPWV distribution, and the filter bank. This section compares the muscle fatigue indices obtained from the filter bank with those muscle fatigue indices obtained from the spectrogram and SPWV.

Two figures of merit were used to quantify the comparison between the muscle fatigue indices computed from the filter bank with the muscle fatigue indices computed from either the spectrogram or SPWV distribution. The first figure of merit was the relative quadratic difference defined as

$$\alpha = \frac{\sum_{n=1}^{L}[s_{fb}(n) - s_{tf}(n)]^2}{\sum_{n=1}^{L}[s_{fb}(n)]^2} \times 100, \tag{3.1}$$

where $s_{fb}(n)$ is either the F_{IMF} or the F_{IA} values at time n estimated from the filter bank, and $s_{tf}(n)$ is either F_{IMF} or the F_{IA} values at time n estimated from either the spectrogram or the SPWV ditribution.

The second figure of merit was the Pearson's correlation coefficients defined as

$$\rho = \frac{1}{L\,\sigma_{fb}\,\sigma_{tf}} \sum_{n=1}^{L} \left[s_{fb}(n) - \overline{s}_{fb}\right] \left[s_{tf}(n) - \overline{s}_{tf}\right], \tag{3.2}$$

where σ_{fb}, and $\overline{s}_{fb}$ are the standard deviations and the sample means, respectively, of either the F_{IMF} or the F_{IA} computed from the filter bank. The parameters σ_{tf}, and $\overline{s}_{tf}$ are the standard deviations and the sample means, respectively, of either the F_{IMF} or the F_{IA} computed from either the spectrogram or the SPWV distribution. The relative quadratic difference is computed for $n = 1, 2, \ldots, L$, where L is the total number of muscle fatigue indices that were computed over a time interval of the estimated IMF or IA.

The following two figures show that the muscle fatigue indices obtained from the filter bank have the same trend as those given by the standard spectrogram and SPWV distribution. Figures 3.1 and 3.2 illustrate the extraction of the F_{IMF} and the F_{IA} of a typical surface EMG signal recorded from the left Splenius at the end of the fifth and sixth hour when the subject was performing an exertion of 70% MVC. Figure 3.1 (a) shows three-minutes surface EMG recording at the end of the fifth hour. Figure 3.1 (b) shows the IMF and IA surface EMG variables that were estimated using the spectrogram, SPWV distribution, and filter bank. Finally, Fig. 3.1 (c) shows the F_{IMF} and the F_{IA} that were estimated using the spectrogram, SPWV distribution, and filter bank. Figure 3.2 (a) shows three-minutes surface EMG recording at the end of the sixth hour. Figure 3.2 (b) shows the IMF and IA surface EMG variables that were estimated using the spectrogram, SPWV

distribution, and filter bank. Finally, Fig. 3.2 (c) shows the F_{IMF} and the F_{IA} that were estimated using the spectrogram, SPWV distribution, and filter bank. Figures 3.1 (c) and 3.2 (c) show that the three methods provide equivalent muscle fatigue indices; e.g., the three methods follow the same trend.

Figures 3.3 and 3.4 illustrate the extraction of the F_{IMF} and the F_{IA} of a typical surface EMG signal recorded from the left Splenius after the third and seventh hour when the subject was performing an exertion of 70% MVC. Figure 3.3 (a) shows the three-minutes recording signal after the third hour. Figure 3.3 (b) shows the IMF and IA surface EMG variables that were estimated using the spectrogram, SPWV distribution, and filter bank. Finally, Figure 3.3 (c) shows the F_{IMF} and the F_{IA} that were estimated using the spectrogram, SPWV distribution, and filter bank. Figure 3.4 (a) shows the three-minutes recording signal after the seventh hour. Figure 3.4 (b) shows the IMF and IA surface EMG variables that were estimated using the spectrogram, SPWV distribution, and filter bank. Finally, Figure 3.4 (c) shows the F_{IMF} and the F_{IA} that were estimated using the spectrogram, SPWV distribution, and filter bank. Figures 3.3 (c) and 3.4 (c) shows that the three methods provide different muscle fatigue indices, as well as different IMF and IA estimates. This difference in the resulting muscle fatigue indices may be caused by wrong signal acquisition. The high amplitude peaks shown in Figs. 3.3 (a) and 3.4 (a) are typical of wrong signal acquisition that are probably caused by poor electrodes placement or bad electrode contact with the subject's skin.

The resulting relative quadratic difference computed for 3480 surface EMG signals are summarized in Table 3.1. In the case of the F_{IMF} computed with the filter bank, 96% had differences not greater than 0.5% compared to those F_{IMF} given by the spectrogram, and 90% had differences not greater than 0.5% compared to those F_{IMF} given by the SPWV distribution. In the case of the F_{IA} computed with the filter bank, 99% had differences not greater than 0.5% compared to those F_{IA} given by the spectrogram, and 100% had differences not greater than 0.5% compared to those F_{IA} given by the SPWV distribution.

The resulting Pearson's correlation coefficients computed for 3480 surface EMG signals are summarized in Table 3.2. Note that a correlation coefficient of one means that the muscle fatigue indices derived from the spectrogram and the SPWV distribution follow the same trend as the

muscle fatigue indices derived from the filter bank. In the case of the F_{IMF} computed with the filter bank, 94% had correlation coefficients greater than 0.9 compared to those F_{IMF} given by the spectrogram, and 88% had correlation coefficients greater than 0.9 compared to those F_{IMF} given by the SPWV distribution. In the case of the F_{IA} computed with the filter bank, 97% had correlation coefficients greater than 0.9 compared to those F_{IA} given by the spectrogram, and 100% had correlation coefficients greater than 0.9 compared to those F_{IA} given by the SPWV distribution.

Cohen has limited the use of wavelets and filter bank in time-frequency analysis. Physical quantities derived from time-frequency distribution (e.g., the first order moment of the frequency distribution) are meaningless or sometimes do not exist [Deb03]. We noted that muscle fatigue indices derived from the spectrogram and the SPWV distribution show not only identical trends but also similar values to those muscle fatigue indices derived from the filter bank. For a few number of muscle fatigue indices, 3% of the results, neither the filter bank, the spectrogram, or the SPWV distribution show equivalent muscle fatigue indices. This is because a wrong signal acquisition causes high localized peaks in some time samples, which can lead to invalid muscle fatigue indices, mainly in the case of the F_{IMF} as shown in Figs. 3.3 and 3.4.

Table 3.1 Relative quadratic difference α of the IMF and IA muscle fatigue indices obtained from the spectrogram, SPWV distribution, and filter bank during the analysis of 3480 surface EMG signals.

Method	$\%$ of F_{IMF} with $\alpha \leq 0.5\%$	$\%$ of F_{IA} with $\alpha \leq 0.5\%$
Spectrogram $\times$ Filter Bank	96	99
SPWV $\times$ Filter Bank	90	100

3.2 Muscle Fatigue Indices

In this section, we assess muscle fatigue from surface EMG signals recorded during isometric voluntary contractions. The surface EMG signals, recorded at 70% MVC, were analyzed when

Table 3.2 Pearson's correlation coefficient ρ of the IMF and IA muscle fatigue indices obtained from the spectrogram, SPWV, and filter bank during the analysis of 3480 SEMG signals.

Method	% of F_{IMF} with $\rho > 0.9$	% of F_{IA} with $\rho > 0.9$
Spectrogram $\times$ Filter Bank	94	97
SPWV $\times$ Filter Bank	88	100

the subject wore helmets A (3.0 Lb baseline) and E (6.0 Lb forward head). Subsection 3.2.1 shows four experimental results, each one corresponding to a different muscle activity region. Subsection 3.2.2 correlates the muscle fatigue indices obtained in the muscle fatigue analysis with the perceived levels of discomfort reported by the subject at the end of the second, fourth, and sixth hour.

3.2.1 Muscle Activity Regions

The following four experimental results show each muscle activity region: muscle increase force, muscle recovery, muscle decrease force, and muscle fatigue. For illustration purposes, we show only four experimental results obtained from the muscle fatigue analysis of a female subject. However, this analysis was performed for the whole 3480 surface EMG signals.

Muscle Increase Force

Muscle increase force assumes that the IMF and the IA increase during the muscle contraction. Figure 3.5 shows muscle increase force in the analysis of a female subject when wearing helmet E. The analyzed surface EMG signal was recorded from the left Trapezius at the end of the fourth hour. In this analysis, we obtained negative F_{IMF} and F_{IA} values. This means that both the IMF and IA are increasing during the whole muscle contraction. On one hand, the F_{IMF} curve increases over time; the IMF increase rate is fast at the onset of the contraction and then is slow at the end of the contraction. On other hand, the F_{IA} curve decreases over time; the IA increase rate is slow at the onset of the contraction and then fast at the end of the contraction. For this particular signal, we identify muscle increase force with the following intensities $\hat{F}_{IMF} = -11.73$ and $\hat{F}_{IA} = -5.26$.

Muscle Recovery

Muscle recovery assumes that the IMF increases and the IA decreases during the muscle contraction. Figure 3.6 shows muscle recovery in the analysis of a female subject when wearing helmet A. The analyzed surface EMG signal was recorded from the left Splenius at the end of the sixth hour.

It is illustrated in Fig. 3.6 that the F_{IMF} is negative during the first 120 s and then becomes positive until the end of the contraction. Also, note that the F_{IMF} curve is increasing during the whole three-minutes recording. These results imply that the IMF increase rate decreases from the onset of the contraction until the time 120 s. After this time the IMF decrease rate continuously increases until the end of the muscle contraction.

In the case of the IA, Fig. 3.6 shows that the F_{IA} is positive, and the F_{IA} curve continuously decreases during the three-minutes recording. These results imply that the IA increases during the whole muscle contraction. Furthermore, the IA increase rate decreases from the onset until the end of the muscle contraction. Analyzing both plots the F_{IMF} and the F_{IA}, we identify two muscle activity regions: (1) there is muscle recovery during the first 120 s because the F_{IMF} is negative (IMF increases) and the F_{IA} is positive (IA decreases); (2) there is muscle increase force after the time 120 s because the F_{IMF} is positive (IMF decreases) and the F_{IA} is positive (IA decreases).

Note that we computed the $\hat{F}_{IMF}$ and $\hat{F}_{IA}$ to identify only one muscle activity region during the whole three-minutes recording. For this particular signal, we identify muscle recovery with the following intensities $\hat{F}_{IMF} = -2.52$ and $\hat{F}_{IA} = 112.6$.

Muscle Decrease Force

Muscle decrease force assumes that the IMF and the IA decrease during the muscle contraction. Figure 3.7 shows muscle decrease force in the analysis of a female subject when wearing helmet A. The analyzed surface EMG signal was recorded from the right Trapezius at the end of the sixth hour.

Figure 3.7 shows that the F_{IMF} and the F_{IA} are positive during the whole muscle contraction. Note that during the three-minutes recording, the F_{IMF} curve is increasing, while the F_{IA} curve

is decreasing. In other words, the IMF decrease rate increases 12%, and the IA decrease rate decreases 3%. For this particular signal, we identify muscle decrease force with the following intensities $\hat{F}_{IMF} = 8.29$ and $\hat{F}_{IA} = 115.26$.

Muscle Fatigue

Muscle fatigue assumes that the IMF decreases and the IA increases during the muscle contraction. Figure 3.8 shows muscle fatigue in the analysis of a female subject when wearing helmet E. The analyzed surface EMG signal was recorded from the left Splenius at the end of the fifth hour.

Figure 3.8 shows an increase in the muscle fatigue curve F_{IMF} and a decrease in the muscle fatigue curve F_{IA}. Note that positive F_{IMF} values correspond to decreases IMF, and negative F_{IA} values correspond to increases IA. Additionally, it is shown in Fig. 3.8 that the IMF decrease rate continuously increases and the IA decrease rate continuously decreases during the whole muscle contraction. These results imply that the muscle fatigue intensity is higher at the end of the contraction than at the onset of the contraction. For this particular signal, we identify muscle fatigue with the following intensities $\hat{F}_{IMF} = 10.89$ and $\hat{F}_{IA} = -123.16$.

3.2.2 Muscle Fatigue Indices Correlation

The computed muscle fatigue indices are correlated to perceived discomfort levels reported by the female subject. The surface EMG signals to be analyzed were recording when the subject wore helmets A (3 Lb baseline CG), B (4.5 Lb near head CG), C (4.5 Lb forward head CG), D (6.0 Lb near head CG), and E (6.0 forward head CG) at the end of the seventh hours. In this subsection, we only correlate the muscle fatigue indices obtained from the analysis of helmets A and E to the perceived discomfort levels reported by the subject at the end of the second, fourth, and sixth hour.

Helmet A

The muscle fatigue indices obtained in the analysis of helmet A inferred that the left and right Splenius are the muscles most fatigued at the end of the second and fourth hour. We obtained at

the end of the second hour a muscle fatigue index of ($\hat{F}_{IMF} = 26.55, \hat{F}_{IA} = -69.74$) for the left Splenius and ($\hat{F}_{IMF} = 29.62, \hat{F}_{IA} = -114.65$) for the right Splenius. In addition, we obtained at the end of the fourth hour a muscle fatigue index of ($\hat{F}_{IMF} = 26.61, \hat{F}_{IA} = -229.64$) for the left Splenius and ($\hat{F}_{IMF} = 46.93, \hat{F}_{IA} = -263.12$) for the right Splenius. From these results, we observed that the muscle fatigue indices obtained from the IA are higher in the fourth hour than in the second hour; e.g., the left Splenius provided $\hat{F}_{IA} = -69.74$ in the second hour and $\hat{F}_{IA} = -229.74$ in the fourth hour. Note that the left and right Splenius do not report muscle fatigue at the end of the sixth hour.

Table 3.3 shows the muscle activity regions and their intensities obtained at the end of the second, fourth, and sixth hour. The muscle activity regions at the end of the second hour are (1) muscle fatigue in the left and right Splenius, left Sterno, and left Trapezius, (2) muscle increase force in the right Sterno, (3) muscle decrease force in the right Trapezius. The muscle activity regions at the end of the fourth hour are (1) muscle fatigue in the left and right Splenius and (2) muscle recovery in the left and right Sterno and in the left and right Trapezius. The muscle activity regions at the end of the sixth hour are (1) muscle recovery in the left Splenius and in the left and right Sterno and (2) muscle decrease force in the left and right Trapezius and in the right Splenius.

The perceived discomfort levels reported by the subject for the following regions (head, upper neck, lower neck, shoulders, upper back, lower back) in the second, fourth, and sixth hour are described below:

a. The subject reported at the end of the second and fourth hour (1) no discomfort, no hot spots, and no numbness in any region and (2) no headache, relaxed mental state, alert mental frame of mind, and attentive concentration level.

b. The subject reported at the end of the sixth hour (1) soreness in the head, upper neck, lower neck, shoulders and upper back, (2) discomfort in the lower back, (3) moderate hot spots in all the regions, (4) no numbness in any region, (5) severe headache, slightly tense, tired mental frame of mind, and distracted concentration level.

The perceived levels of discomfort reported in the second, fourth, and sixth hour do not match

the obtained muscle fatigue indices. From the obtained muscle fatigue indices, we expected the subject to report a higher fatigue intensity at the end of the second and fourth hour, rather than at the end of the sixth hour. This is because there are more fatigued muscles at the end of the second and fourth hour than at the end of the sixth hour. Also, note that there are five fatigued muscles at the end of the second hour, and two fatigued muscles at the end of the fourth hour. However, the two-fatigued muscles from the fourth hour have much higher muscle fatigue intensities than the five-fatigued muscles from the second hour.

Table 3.3 Muscle activity regions of a female subject when wearing helmet A at the end of the second, fourth, and sixth hour. Muscle fatigue region in blue and bold face.

	H2		**H4**		**H6**	
Muscles	$\hat{F}_{IMF}$	$\hat{F}_{IA}$	$\hat{F}_{IMF}$	$\hat{F}_{IA}$	$\hat{F}_{IMF}$	$\hat{F}_{IA}$
Left Splenius	**26.55**	**-69.74**	**26.61**	**-229.64**	-2.52	112.60
Left Sterno	**13.87**	**-41.29**	-40.04	53.30	-30.84	106.28
Left Trapezius	**11.63**	**-14.79**	-2.87	21.83	12.91	113.58
Right Splenius	**29.62**	**-114.65**	**46.93**	**-263.12**	3.73	92.40
Right Sterno	-22.75	-12.27	-17.05	32.36	-73.53	137.53
Right Trapezius	16.24	13.92	-8.41	28.88	8.29	115.26

Helmet E

The muscle fatigue indices obtained in the analysis of helmet E inferred that the left and right Splenius are the muscles most fatigued at the end of the second, fourth, and sixth hour. We obtained at the end of the second hour a muscle fatigue index of $(\hat{F}_{IMF} = 30.62, \hat{F}_{IA} = -147.57)$ for the left Splenius, and $(\hat{F}_{IMF} = 23.41, \hat{F}_{IA} = -94.04)$ for the right Splenius. We obtained at the end of the fourth hour a muscle fatigue index of $(\hat{F}_{IMF} = 26.88, \hat{F}_{IA} = -131.87)$ for the left Splenius, and $(\hat{F}_{IMF} = 42.41, \hat{F}_{IA} = -162.92)$ for the right Splenius. Finally, we obtained at the end of the sixth hour a muscle fatigue index of $(\hat{F}_{IMF} = 16.29, \hat{F}_{IA} = -230.00)$ for the left Splenius, and $(\hat{F}_{IMF} = 34.91, \hat{F}_{IA} = -177.44)$ for the right Splenius.

From these results, we observed that the muscle fatigue indices obtained from the IA are higher in the sixth hour than in the fourth and second hour. For instance, the left Splenius provided

$\hat{F}_{IA} = -230.00$) in the sixth hour, $\hat{F}_{IA} = -131.87$) in the fourth hour, and $\hat{F}_{IA} = -147.57$) in the second hour. In addition, the left and right Splenius are fatigued at the end of the second, fourth, and sixth hour. Note that these two muscles are more fatigued at the end of the sixth hour than at the end of the fourth and second hour.

Table 3.4 shows the muscle activity regions and their intensities obtained at the end of the second, fourth, and sixth hour. The muscle activity regions at the end of the second hour are (1) muscle fatigue in the left and right Splenius, (2) muscle increase force in the right Trapezius, (3) muscle recovery in the left and right Sterno and in the left Trapezius. The muscle activity regions at the end of the fourth hour are (1) muscle fatigue in the left and right Splenius and in the left Sterno (2) muscle increase force in the left Trapezius and right Sterno, and (3) muscle recovery in the right Trapezius. Finally, the muscle activity regions at the end of the sixth hour are (1) muscle fatigue in the left and right Splenius and in the left Sterno, (2) muscle recovery in the left Trapezius and right Sterno, and (3) muscle decrease force in the right Trapezius.

Table 3.4 Muscle activity regions of a female subject when wearing helmet E at the end of the second, fourth, and sixth hour. Muscle fatigue region in blue and bold face.

	H2		**H4**		**H6**	
Muscles	$\hat{F}_{IMF}$	$\hat{F}_{IA}$	$\hat{F}_{IMF}$	$\hat{F}_{IA}$	$\hat{F}_{IMF}$	$\hat{F}_{IA}$
Left Splenius	**30.62**	**-147.57**	**26.88**	**-131.87**	**16.29**	**-230.00**
Left Sterno	-15.79	9.34	**4.59**	**-12.71**	**27.27**	**-24,86**
Left Trapezius	-2.66	19.92	-11.73	-5.26	-23.67	17.45
Right Splenius	**23.41**	**-94.09**	**42.41**	**-162.92**	**34.91**	**-177.41**
Right Sterno	-3.85	4.86	-8.15	-5.98	-11.96	63.53
Right Trapezius	-0.15	-24.29	-32.00	63.83	27.77	2.24

The perceived discomfort levels reported by the subject for the following regions (head, upper neck, lower neck, shoulders, upper back, lower back) after the second, fourth, and sixth hour are described below:

a. The subject reported at the end of the second hour (1) discomfort, moderate hot spots, and no numbness in all the regions, (2) minimal headache, slightly tense, tired mental frame of

mind, and attentive concentration level.

b. The subject reported at the end of the fourth hour (1) soreness, moderate hot spots, and no numbness in all the regions, (2) severe headache, slightly tense, tired mental frame of mind, and distracted concentration level.

c. The subject reported at the end of the sixth hour (1) pain in, severe hot spots, and no numbness in all the regions and (2) severe headache, restless, exhausted mental frame of mind, and loss of focus.

The perceived levels of discomfort reported at the end of the second, fourth, and sixth hour match the obtained muscle fatigue indices. The number and the intensity of fatigued muscles were increased in each hour. Moreover, there are two fatigued muscles at the end of the second hour, and three fatigued muscles at the end of the fourth and sixth hour. The muscle fatigue intensities were much higher in the fatigued muscles from the sixth hour than the fatigued muscles from the fourth and second hour.

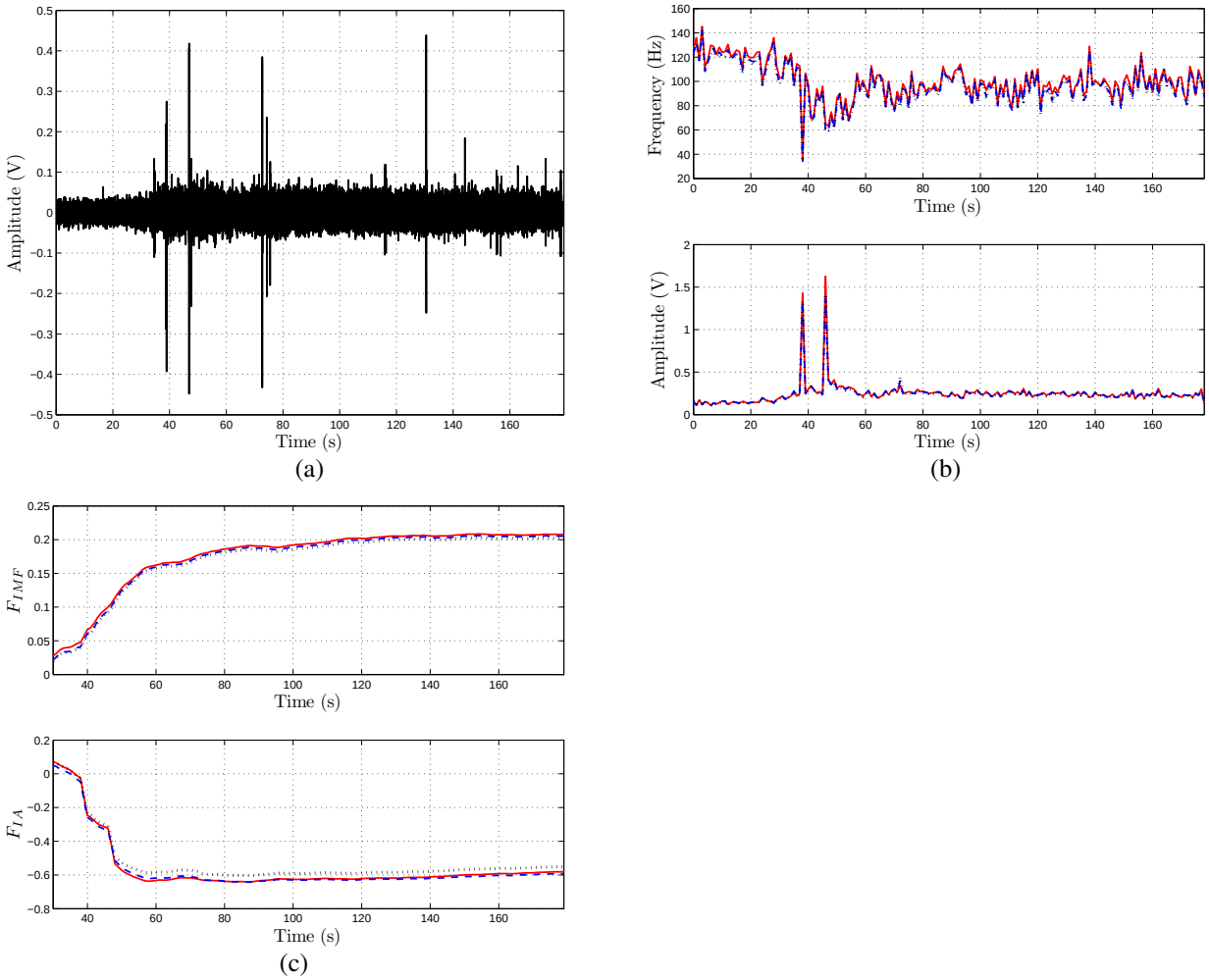

Figure 3.1 Surface EMG signal recorded at the end of the fifth hour without noise. Correct estimation of their IMF and IA, and correct estimation of their F_{IMF} and F_{IA}. The subject wore helmet A during the 70% MVC. (a) three-minutes surface EMG signal recording from the left Splenius, (b) estimated IMF and IA, (c) estimated F_{IMF} and F_{IA}. Methods – spectrogram (dashed blue line), SPWV (dotted black line), and filter bank (continuous red line) –. The IMF and IA estimates, as well as the F_{IMF} and F_{IA} show similar trends and values for the three methods.

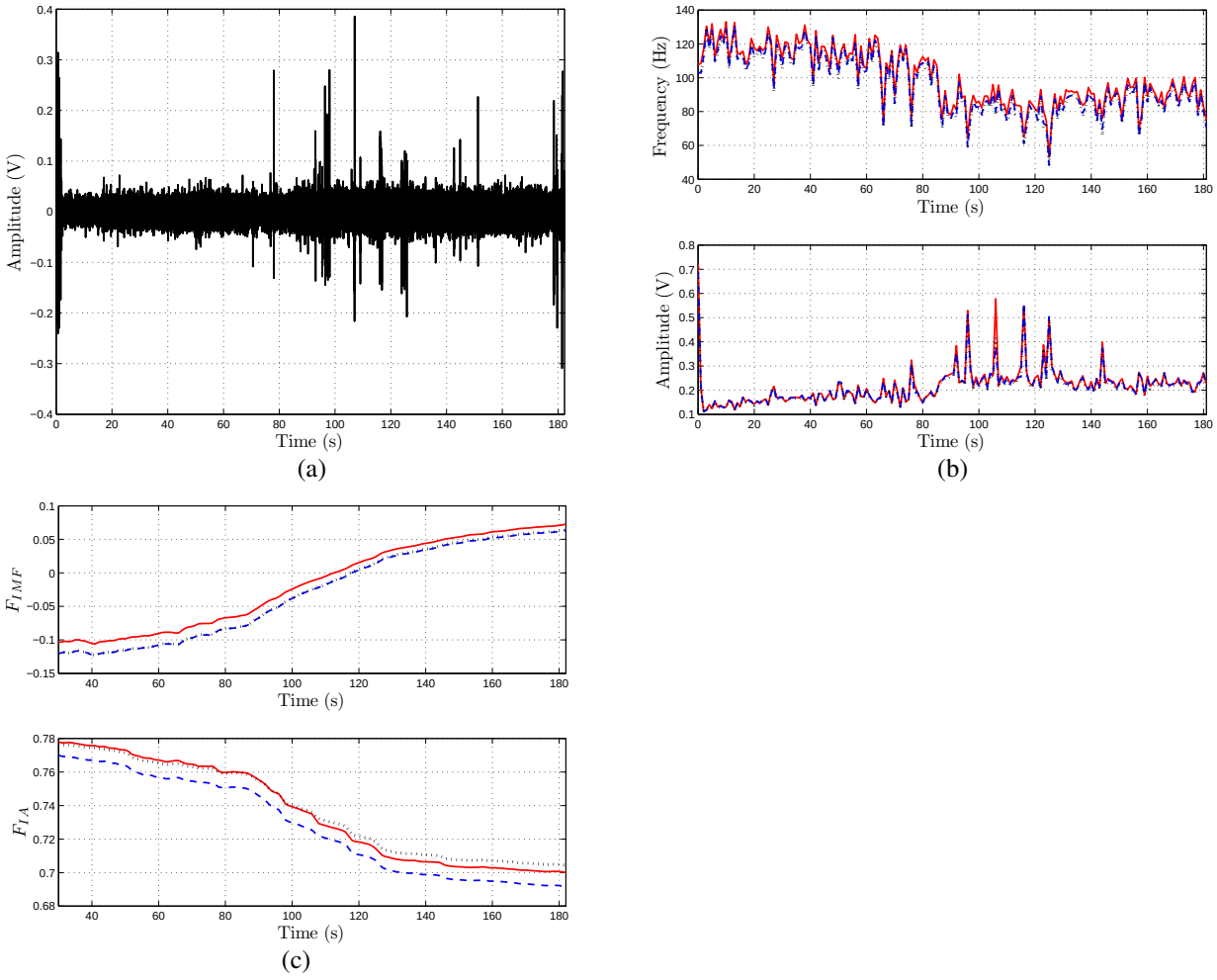

Figure 3.2 Surface EMG signal recorded at the end of the sixth hour without noise. Correct estimation of their IMF and IA, and correct estimation of their F_{IMF} and F_{IA}. The subject wore helmet A during the 70% MVC. (a) three-minutes surface EMG signal recording from the left Splenius, (b) estimated IMF and IA, (c) estimated F_{IMF} and F_{IA}. Methods – spectrogram (dashed blue line), SPWV (dotted black line), and filter bank (continuous red line) –. The IMF and IA estimates, as well as the F_{IMF} and F_{IA} show similar trends and values for the three methods.

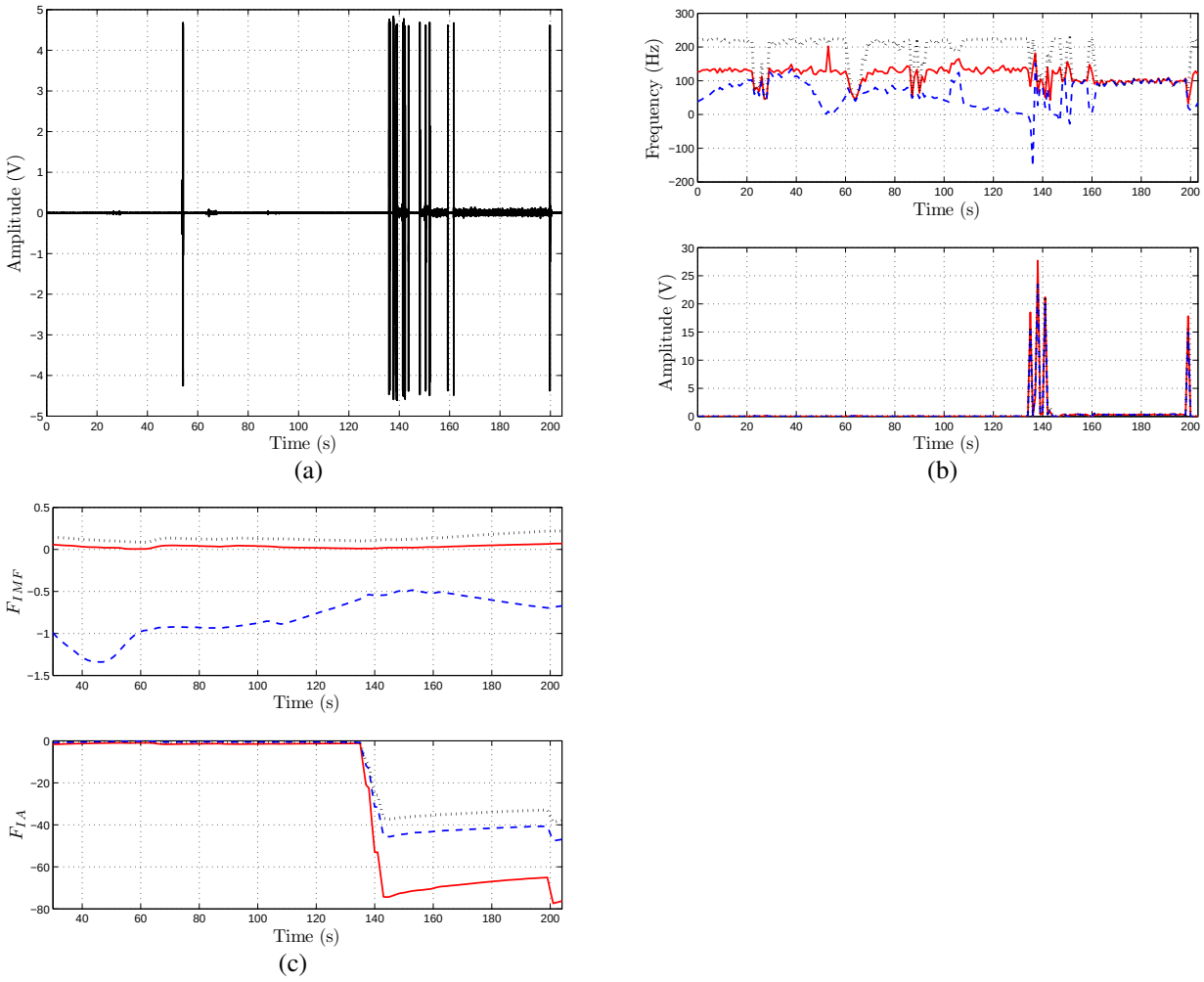

Figure 3.3 Surface EMG signal recorded at the end of the third hour with noise. Wrong estimation of their IMF and IA, and wrong estimation of their F_{IMF} and F_{IA}. The subject wore helmet E during the 70% MVC. (a) three-minutes surface EMG signal recording from the left Splenius, (b) estimated IMF and IA, (c) estimated F_{IMF} and F_{IA}. Methods – spectrogram (dashed blue line), SPWV (dotted black line), and filter bank (continuous red line) –. The IMF and IA estimates, as well as the F_{IMF} and F_{IA} show similar trends and values for the three methods.

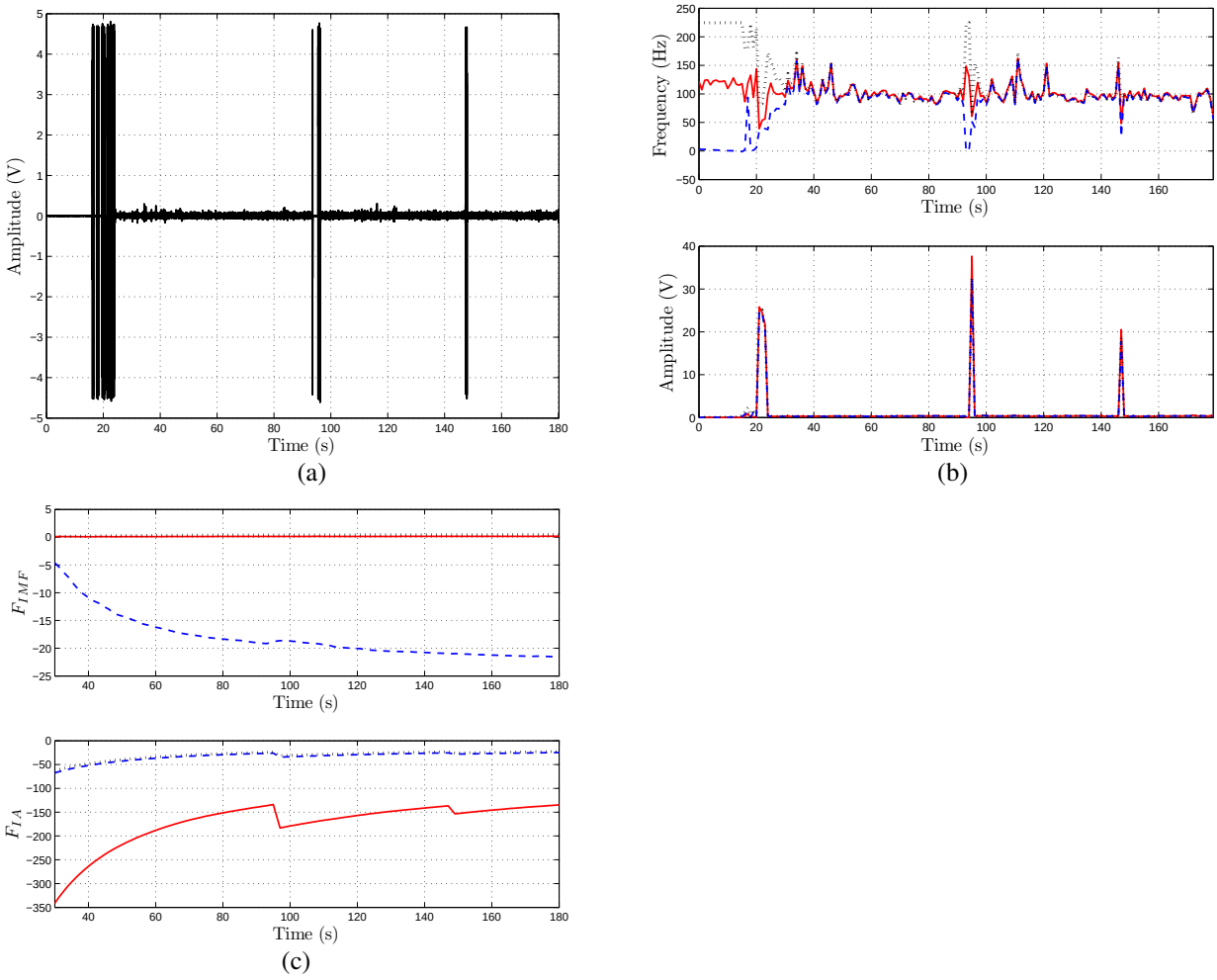

Figure 3.4 Surface EMG signal recorded at the end of the seventh hour with noise. Wrong estimation of their IMF and IA, and wrong estimation of their F_{IMF} and F_{IA}. The subject wore helmet E during the 70% MVC. (a) three-minutes surface EMG signal recording from the left Splenius, (b) estimated IMF and IA, (c) estimated F_{IMF} and F_{IA}. Methods – spectrogram (dashed blue line), SPWV (dotted black line), and filter bank (continuous red line) –. The IMF and IA estimates, as well as the F_{IMF} and F_{IA} show similar trends and values for the three methods.

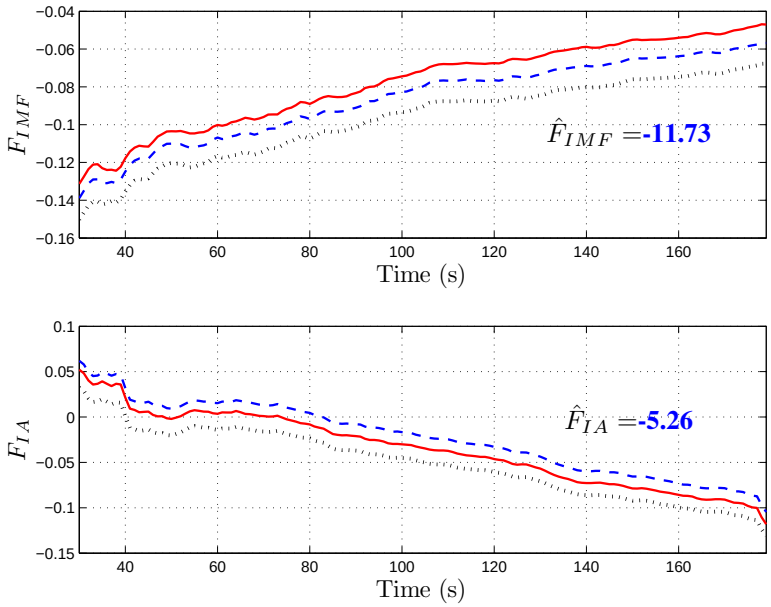

Figure 3.5 Muscle activity indices for the left Trapezius analysis at the end of the fourth hour when the subject wore helmet E. In general the muscle presents increase force during the whole contraction. On the top is shown the muscle activity indices computed from the IMF (F_{IMF}). On the bottom is shown the muscle activity indices computed from the IA (F_{IA}). In blue, bold face are the intensities $\hat{F}_{IMF}$, and $\hat{F}_{IA}$. Methods – spectrogram (dashed blue line), SPWV (dotted black line), and filter bank (continuous red line) –.

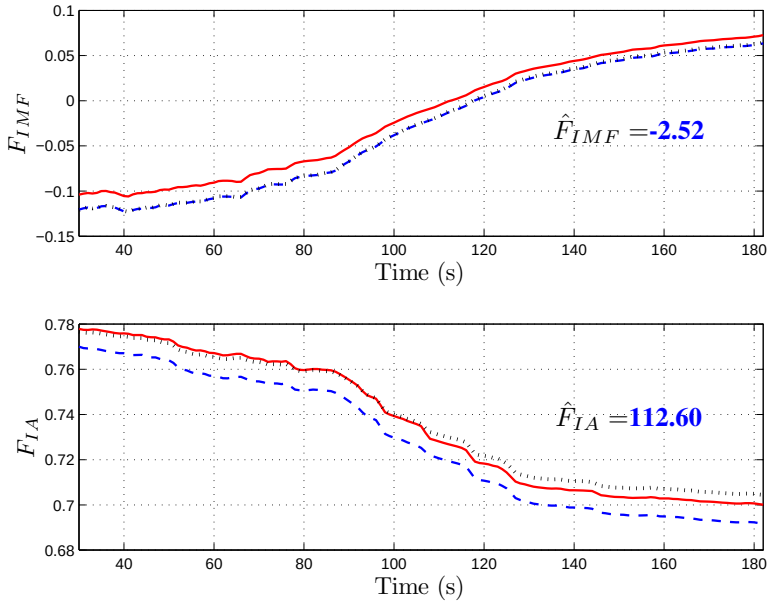

Figure 3.6 Muscle activity indices for the left Splenius analysis at the end of hour 6 when the subject wore helmet A. In general the muscle presents recovery during the whole contraction. On the top is shown the muscle activity indices computed from the IMF (F_{IMF}). On the bottom is shown the muscle activity indices computed from the IA (F_{IA}). In blue, bold face are the intensities $\hat{F}_{IMF}$, and $\hat{F}_{IA}$. Methods – spectrogram (dashed blue line), SPWV (dotted black line), and filter bank (continuous red line) –.

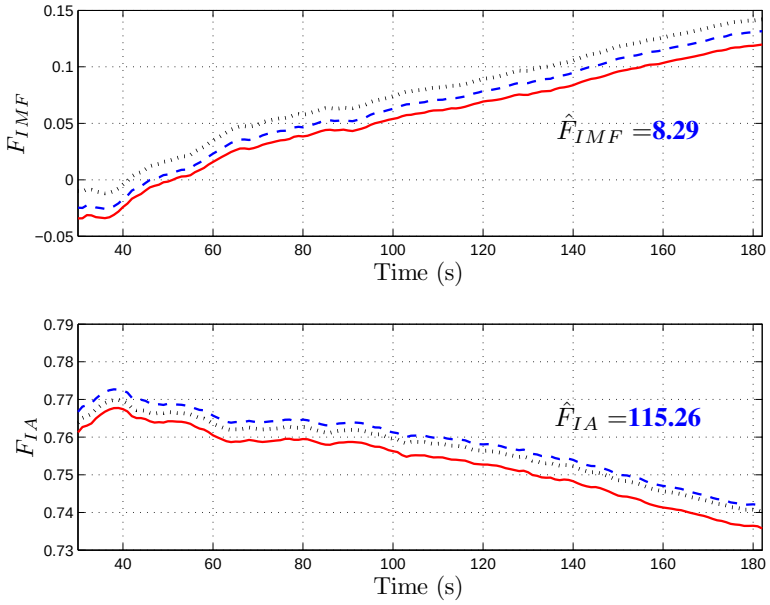

Figure 3.7 Muscle activity indices for the right Trapezius analysis at the end of hour 6 when the subject wore helmet A. In general the muscle presents recovery during the whole contraction. On the top is shown the muscle activity indices computed from the IMF (F_{IMF}). On the bottom is shown the muscle activity indices computed from the IA (F_{IA}). In blue, bold face are the intensities $\hat{F}_{IMF}$, and $\hat{F}_{IA}$. Methods – spectrogram (dashed blue line), SPWV (dotted black line), and filter bank (continuous red line) –.

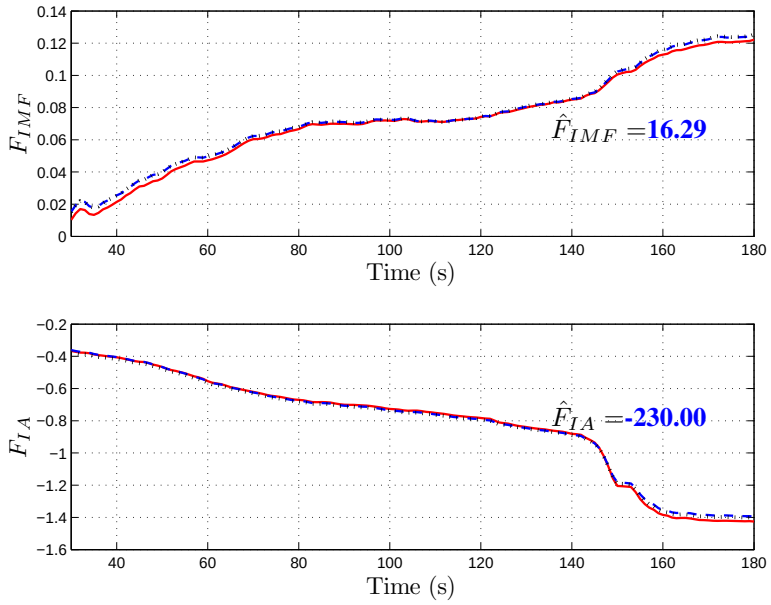

Figure 3.8 Muscle activity indices for the left Splenius analysis at the end of the sixth hour when the subject wore helmet E. The muscle presents fatigue during the three-minutes recording. On the top is shown the muscle activity indices computed from the IMF (F_{IMF}). On the bottom is shown the muscle activity indices computed from the IA (F_{IA}). In blue, bold face are the intensities $\hat{F}_{IMF}$, and $\hat{F}_{IA}$. Methods – spectrogram (dashed blue line), SPWV (dotted black line), and filter bank (continuous red line) –.

4
Conclusion

This project aims to measure human muscle fatigue from surface electromyographic (EMG) signals recorded during isometric voluntary contractions. It is well known that during muscle fatigue the force decreases because of neuromuscular physiological changes such as motor unit recruitment, lactic acid, and pH. Lactic acid accumulation and pH decrements in the muscle cells are two crucial factors during muscle fatigue.

Surface EMG variables such as frequency, muscle fiber conduction velocity, and amplitude are very sensitive to these physiological changes; e.g. frequency and muscle fiber conduction velocity decreases are attributed to lactic acid accumulation and a lower pH. In addition, amplitude increases have been reported during force increases and muscle fatigue due to increases in the recruitment of motor units. In this work, we assume that the frequency decreases and the amplitude increases during muscle fatigue. This is because the surface EMG signals were recorded during isometric voluntary contractions.

To estimate the instantaneous mean frequency (IMF) and the instantaneous amplitude (IA), we propose a technique where the surface EMG signal is decomposed of 32 subbands by using a cosine modulated filter bank. The proposed method (filter bank) has the advantage of being window independent and provides a better cross term suppression than the other evaluated techniques (spectrogram and smoothed pseudo Wigner-Ville (SPWV) distribution). In addition, the filter bank can be implemented by iterating a two channel filter bank used to compute the wavelet coefficients of the surface EMG signal in a scheme also known as wavelet packets. The advantage of using a wavelet decomposition is that the estimation of the IMF and IA can be combined with other techniques based on wavelet transforms such as baseline drift removal and signal noise reduction.

The IMF is estimated from the subbands of the filter bank as the first order moment of the

frequency distribution at a certain point in time. The IA is estimated from the subbands of the filter bank, according to a proposed technique based on applying the outputs of the filters to successive, overlapping adaptive windows and determining the maximum coefficient from each window. The sum of the maximum coefficients for the different subbands corresponds to a single IA estimate.

For evaluating the IMF and IA slopes computed from the filter bank decomposition, two other standard techniques, the spectrogram and the SPWVD, were also implemented since they were shown to provide a better estimation of the IMF and IA than the Wigner-Ville distribution and the Choi-Williams distribution. From the spectrogram and the SPWVD, the IMF was also estimated as the first order moment of the frequency distribution at a certain point of time, and the IA was estimated as the squared root of the time marginal.

After having estimated the IMF and IA, we computed a regression-free EMG index F for time intervals of 30 s. If the surface EMG variable shows a decrease pattern then $0 \leq F \leq 1$, and if the surface EMG variable shows an increase pattern then $F \leq 0$. We called F_{IMF} to the EMG index obtained from the IMF, and F_{IA} to the EMG index obtained from the IA. In addition, we called $\hat{F}_{IMF}$ and $\hat{F}_{IA}$, respectively, to the quantities computed by integrating the F_{IMF} and F_{IA} over the three-minutes recording.

By using a joint analysis of spectrum and amplitude (JASA), the $\hat{F}_{IMF}$ and $\hat{F}_{IA}$ quantities obtained from the spectrogram, SPWV distribution, and filter bank were classified into one of the following four muscle activity regions: (1) muscle increase force when both the $\hat{F}_{IMF}$ and $\hat{F}_{IA}$ are negative; (2) muscle recovery when the $\hat{F}_{IMF}$ is negative and the $\hat{F}_{IA}$ is positive; (3) muscle decrease force when both the $\hat{F}_{IMF}$ and $\hat{F}_{IA}$ are positive; and (4) muscle fatigue when the $\hat{F}_{IMF}$ is positive and $\hat{F}_{IA}$ is negative. The pair $\hat{F}_{IMF}, \hat{F}_{IA}$ is proposed as an index to measure the intensity level of muscle increase force, muscle recovery, muscle decrease force, and muscle fatigue. During the performance tests, the F_{IMF} and F_{IA} were computed from the filter bank, the spectrogram, and the SPWV distribution of 3480 surface EMG signals provided by the Air Force Research Lab. F_{IMF} and F_{IA} obtained from the filter bank were correlated and compared to the F_{IMF} and F_{IA} obtained from the spectrogram and the SPWV distribution. In the case of the F_{IMF} computed with the filter bank, 94% showed correlation coefficients greater than 0.9 compared to

those F_{IMF} given by the spectrogram, and 88% showed correlation coefficients greater than 0.9 compared to those F_{IMF} given by the SPWV distribution. In the case of the F_{IA} computed with the filter bank, 97% showed correlation coefficients greater than 0.9 compared to those F_{IA} given by the spectrogram, and 100% showed correlation coefficients greater than 0.9 compared to those F_{IA} given by the SPWV distribution. These results verify that the F_{IMF} and F_{IA} obtained from the filter bank show a strong correlation and the same trend as those given by the standard spectrogram and the SPWV distribution techniques.

The relative quadratic differences, when comparing the F_{IMF} and F_{IA} computed from the filter bank with those F_{IMF} and F_{IA} computed from the spectrogram and the SPWV distribution, showed that 89.6% of the differences were less than 0.5%. The F_{IMF} and F_{IA} obtained from the filter bank not only show the same trend but also close values to those given by the spectrogram and the SPWV distribution.

For a few numbers of F_{IMF} and F_{IA}, 3% of the results obtained from the data, neither the filter bank, the spectrogram, or the SPWV distribution showed equivalent EMG indices. This was attributed to the fact that the corresponding surface EMG signals show high peak values at some samples due to poor placement of the electrodes or bad contact of the electrodes with the subject's skin.

The resulting muscle fatigue indices for each muscle activity region were correlated to the perceived levels of discomfort reported by the subjects. An extensive evaluation of the 3480 surface EMG signals showed that the proposed filter bank decomposition is a suitable tool for determining human muscle fatigue during isometric voluntary contractions. For example, muscle fatigue was analyzed for a subject performing 70% MVC and wearing helmets A and E during an eight-hour session. This analysis showed that the left and right Splenius are the muscles most fatigued when the subject wore helmets A and E. In the case of the helmet A, the perceived levels of discomfort reported by the subject did not match the obtained muscle fatigue indices. On one hand, the subject reported an increase muscle fatigue intensity from the second to the sixth hour. On the other hand, we obtained more fatigued muscles at the end of the second hour than at the end of the fourth and sixth hours. In the case of the helmet E, the perceived levels of discomfort reported by the subject

matched the obtained muscle fatigue indices. The subject reported an increased muscle fatigue intensity from the second to the sixth hour, and we obtained more fatigued muscles with higher muscle fatigue intensities at the end of the sixth hour than at the end of the second and fourth hours.

A limitation of the experimental results is that the levels of discomfort were reported for certain regions (head, upper neck, lower neck, shoulders, upper back, and lower back) related to the analyzed neck muscles but not specifically for each muscle. Moreover, the discomfort levels are characteristic of the subject and can change depending on the mood, time, weather, and other factors that are involved during the collection of the surface EMG signals. Therefore, it is important to correlate surface EMG signals to other biomedical measurements such as blood sample, heart rate, and electroencephalographic (EEG) signals in order to create a more reliable index to measure the intensity of muscle fatigue felt by the subject. Furthermore, our proposed method should be extended to the muscle fatigue analysis of surface EMG signals recorded during dynamic voluntary contractions.

References

[AHJDR86] P. Astrand, E. Hultman, A. Juhlin-Dannfelt, and G. Reynolds. Disposal of lactate during and after strenuous exercise in humans. *Journal of Applied Physiology*, 61:338–343, 1986.

[BA07] V. Balasubramanian and K. Adalarasu. EMG-based analysis of change in muscle activity during simulated driving. *Journal of Bodywork and Movement Therapies*, 11:151–158, 2007.

[BGK96] P. Bonato, G. Giagliati, and M. Knaflitz. Analysis of myoelectric signals recorded during dynamic contractions. *IEEE Engineering in Medicine and Biology*, pages 102–111, 1996.

[BPR+91] L. R. Brody, M. T. Pollocks, S. H. Roy, C. J. De Luca, and B. Celli. ph-induced effects on median frequency and conduction velocity of the myoelectric signal. *Journal of Applied Physiology*, 71:1878–1885, 1991.

[BRKL01] P. Bonato, S. H. Roy, M. Knaflitz, and C. J. De Luca. Time-frequency parameters of the surface myoelectric signal for assesing muscle fatigue during cyclic dynamic contractions. *IEEE Transactions on Biomedical Engineering*, 48:745–753, 2001.

[Coh95] L. Cohen. *Time-Frequency Analysis*. Prentice Hall Signal Processing Series, 1995.

[DDMM95] J. Duchene, D. Devedeux, S. Mansour, and C. Marque. Analyzing uterine EMG: Tracking instantaneous burst frequency. *IEEE Engineering in Medicine and Biology*, pages 125–132, 1995.

[Deb03] Lokenath Debnath, editor. *Wavelets and Signal Processing*. Birkhauser, 2003.

[FdL82] S. Foster and C. de Luca. Muscle fatigue monitor: A noninvasive device for observing localized muscular fatigue. *IEEE Transactions on Biomedical Engineering*, BME–29:760–768, 1982.

[FM00] D. Farina and R. Merletti. Comparison of algorithms for estimation of emg variables during voluntary isometric contractions. *Journal of Electromyography and Kynesiology*, 10:337–349, 2000.

[Gan01] S. C. Gandevia. Spinal and supraspinal factors in human muscle fatigue. *Physiological Reviews*, 81:1725–1789, 2001.

[GSG03] A. Georgakis, L. K. Stergioulas, and G. Giakas. Fatigue analysis of the surface EMG signal in isometric constant force contractions using the averaged instantaneous frequency. *IEEE Transactions on Biomedical Engineering*, 50:262–265, 2003.

[HAO06] N. E. Huang and N. O. Attoh-Okine, editors. *The Hilber-Huang Transform in Engineering*. CRC Press, 2006.

[KAFH07] G. Kim, M. A. Ahad, M. Ferdjallah, and G. F. Harris. Correlation of muscle fatigue indices between intramuscular and surface EMG signals. *SoutheastCon, 2007. Proceedings. IEEE*, pages 378–382, 2007.

[KG04] J. Kilby and H. Gholam. Wavelet analysis of surface electromyography signals. *Proceedings of the 26th Annual International Conference of the IEEE/EMBS*, pages 384–387, 2004.

[KGa01] S. Karlsson, B. Gerdle, and M. akay. Analyzing surface myoelectric signals recorded during isokinetic contractions. *IEEE Engineering in Medicine and Biology*, pages 97–105, 2001.

[Kon05] P. Konrad. The abc of emg, 2005.

[KPB03] D. K. Kumar, N. D. Pah, and A. Bradley. Wavelet analysis of surface electromyography to determine muscle fatigue. *IEEE Transactions on Neural Systems and Rehabilitation Engineering*, 11:400–406, 2003.

[KT79] P. V. Komi and P. Tesch. Emg frequency spectrum, muscle structure, and fatigue during dynamic contractions in man. *European Journal of Applied Physiology*, 42:41–50, 1979.

[KYA98] S. Karlsson, J. Yu, and M. Akay. Spectral analysis of myoelectric signals by wavelet methods. *2nd International Conference on Bioelectromagnetism*, pages 33–34, 1998.

[LJL00a] A. Luttmann, M. Jager, and W. Laurig. Electromyographical indication of muscular fatigue in occupational field studies. *International Journal of Industrial Ergonomics*, pages 645–660, 2000.

[LJL00b] A. Luttmann, M. Jager, and W. Laurig. Electromyographical indication of muscular fatigue in occupational field studies. *International journal of Industrial ergonomics*, pages 645–660, 2000.

[LJSL96] A. Luttmann, M. Jager, J. Sokeland, and W. Laurig. Electromyographical study on surgeons in urology. ii. determination of muscular fatigue. *Ergonomics*, 39:298–313, 1996.

[LKP77] L. Lindstrom, R. Kadefors, and I. Petersen. An electromyographic index for localized muscle fatigue. *Journal of Applied Physiology*, 43:750–754, 1977.

[MCO90] R. Merletti, L. R. Lo Conte, and C. Orizio. Indices of muscle fatigue. *Journal of Electromyography and Kynesiology*, 1:20–33, 1990.

[MP04] R. Merletti and P. A. Parker. *Electromyography: Physiology, Engineering, and Noninvasive Applications*. IEEE Press Series in Biomedical Engineering, 2004.

[PB97] J. R. Potvin and L. R. Bent. A validation of techniques using surface emg signals from dynamic contractions to quantify muscle fatigue during repetitive tasks. *Journal of Electromyography, Kynesiology*, 7:131–139, 1997.

[PS03] A. Papandreou-Suppappola, editor. *Applications in Time-Frequency Signal Processing*. CRC Press, 2003.

[PvdMB06] J.B. Prins, J. W. van der Meer, and G. Bleijenberg. Chronic fatigue syndrome. *The Lancet*, 367:346–355, 2006.

[RA97] C. U. Ranniger and D. L. Akin. EMG mean power frequency determination using wavelet analysis. *Proceedings of the 19th IEEE/EMBS*, pages 1589–1592, 1997.

[RM04] P. A. Parker R. Merletti. *Electromyography: Physiology, Engineering, and Noninvasive Applications*. IEEE Press Series in Biomedical Engineering, 2004.

[Sch98] Kansas University Medical School. Thcme medical biochemistry – biochemistry subject list, April 1998.

[Sch05] Harvard Medical School, editor. *Boosting Your Energy*. Harvard Health Publications, 2005.

[SK00] M. Akay S. Karlsson, J. Yu. Time-frequency analysis of myoelectric signals during dynamic contractions: A comparative study. *IEEE Transactions on Biomedical Engineering*, 47:228–238, 2000.

[SPBJ00] P. J. Sparto, M. Parnianpour, E. A. Barria, and J. M. Jagadeesh. Wavelet and short-time fourier transform analysis of electromyography for detection of back muscle fatigue. *IEEE Transactions on Rehabilitation Engineering*, 8:433–436, 2000.

[TKK+05] L. Trejo, R. Kochavi, K. Kubitz, L. Montgomery, R. Rosipal, and B. Matthews. EEG-based estimation of cognitive fatigue. In *Proceedings of SPIE Vol. 5797: Biomonitoring for Physiological and Cognitive Performance During Military Operations, SPIE Defense & Security Symposium*, pages 105–115, Orlando, FL, 2005.

[Tsc00] V. Tscharner. Intensity analysis in time-frequency space of surface myoelectric signals by wavelets of specified resolution. *Journal of electromyography and kynesiology*, pages 433–445, 2000.

[XW06] H. Xie and Z. Wang. Mean frequency derived via hilbert-huang transform with application to fatigue EMG signal analysis. *Computer Methods and Programs in Biomedicine*, 82:114–120, 2006.

[zA05] A. Al zaman and M. A. Ahad. A new approach for muscle fatigue analysis in young adults at different MVC levels. *IEEE*, 1:499–502, 2005.

[ZASF07] A. Al Zaman, M. Ashraf, T. Sharmin, and M. Ferdjallah. Muscle fatigue analysis in young adults at different mvc levels using emg metrics. *IEEE*, pages 390–394, 2007.

[ZBvE08] M. J. Zwarts, G. Bleijenberg, and B. G. M. van Engelen. Clinical neurophysiology of fatigue. *International Federation of Clinical Neurophysiology*, 119:2–10, 2008.

[zFK06] A. Al zaman, M. Ferdjallah, and A. Khamayseh. Muscle fatigue analysis for healthy adults using TVAR model with instantaneous frequency estimation. *Proceedings of the 38th Southeastern Symposium on System Theory*, pages 44–47, 2006.

A
Toolbox

Algorithm 1 Compute the Instantaneous Mean Frequency and the Instantaneous Amplitude

Input:

- Define the signal $x[n]$, $\forall\, n = 0, 1, 2, 3, \ldots, L-1$, where L is the length of the signal
- Define a filter bank $h[f, n]$, $\forall\, n = 0, 1, 2, 3, \ldots, M-1$ and $f = 0, 1, 2, 3 \ldots, F-1$, where M is the length of each filter and F is the number of subbands. The filter f_0 is a low pass filter and the filter f_{F-1} is a high pass filter. In this tool box all the filters have the same length

Output:

- Instantaneous frequency $\hat{f}[n]$
- Instantaneous amplitude $i_a[n]$

Compute the subband coefficients $\hat{y}[f, n]$ convolving the input $x[n]$ with the filter bank $h[f, n]$; $\hat{y}[f, n] = x[n] * h[f, n]$. The resulting output $\hat{y}[f, n]$ is defined $\forall\, n = 0, 1, 2, 3, \ldots, L + M - 2$ and $f = [0, 1, 2, 3, \ldots, F-1]\frac{1}{2F}$

Define the output $y[f, n]$ as
$y[f, n] = \hat{y}[f, n + \frac{M}{2}]$, $\forall\, n = 0, 1, 2, 3, \ldots, L-1$

Compute the time subband representation as
$y[f, n] = (y[f, n])^2$

Compute the time marginal $m[n]$ as

$$m[n] = \sum_{f=0}^{F-1} y[f, n]$$

Compute the instantaneous frequency $\hat{f}[n]$ as

$$\hat{f}[n] = \frac{\sum_{f=0}^{F-1} f y[f, n]}{m[n]}$$

Compute the instantaneous amplitude $i_a[n]$ as

for $f = 0$ to $F - 1$ **do**
  $\tau = \text{ceil}(\frac{2F}{f+1})$, $k = 0$, flag$= 1$
  while flag$\neq 0$ **do**
    $s_{f,k}[n] = y[f, n + k]$; $\forall\, n = 0, 1, 2, 3, \ldots, \tau - 1$
    $\psi[f, k] = \max(s_{f,k}[n])$
    $r = L + M - 1 - k$
    if $r = 0$ **then**
      $flag = 0$
    else
      $k = k + 1$
    end if
  end while
end for

$$i_a[n = k] = \sum_{f=0}^{F-1} \psi[f, k]$$

Matlab Functions Content

The following functions shown in Table A.1 are implemented in Matlab. These functions are used in this research to assess muscle fatigue.

Table A.1 Matlab functions used in the assessment of muscle fatigue.

Matlab Function	Purpose
gfb	Generate the analysis filter bank
f_filter_bank_ana	Compute the subband outputs of the filter bank
tsub	Arrange all the computed subband coefficients in a matrix form
inst_freq	Compute the instantaneous mean frequency of a given signal
inst_amp	Compute the instantaneous amplitude of a given signal
windowing	Compute the start and end indices of the location of a rectangular moving window
fatigue_index	Compute the index of a given surface EMG variable

gfb

Purpose

Generate the analysis filter bank.

Synopsis

```
[fltana, indfltana]=gfb(n_sb)
```

Description

`gfb` generates the analysis filterbank. For this toolbox the number of subbands `n_sb` can be $16, 32$ or 64. We can represent the filterbank in matrix form by $h[f, n]$=`fltana`$(fM_f + n + 1)$ for f=$0, 1, 2, 3, \ldots, F - 1$ and n=$0, 1, 2, 3, \ldots, M_f - 1$ where F is the number of subbands `n_sb` and M_f is the length of the filter in subband f. The length of the filter f can be computed from `indfltana` using M_f=`indfltana`$(f + 1)-$`indfltana`(f) for $f > 0$, and `indfltana`$(f + 1)$ for f=0. The output `indfltana` is required only when the filters have different length. In this project all the filters used had length equal to 128 coefficients.

Name	Description	Default value
`n_sb`	number of subbands	32
`fltana`	column vector with the coefficients of the analysis filter bank	
`indfltana`	column vector with the index of the end of each filter	

Example

```
[fltana, indfltana]=gfb(32);
hn=reshape(fltana,128,32);
Hf=fft(hn,512);
f=linspace(0,511,256);
plot(f,abs(Hf(256:511,:)));
xlabel('f (Hz)', 'fontsize',14,...
'interpreter', 'latex');
ylabel('$|H(f)|$', 'fontsize', 14,...
'interpreter', 'latex'); grid on
```

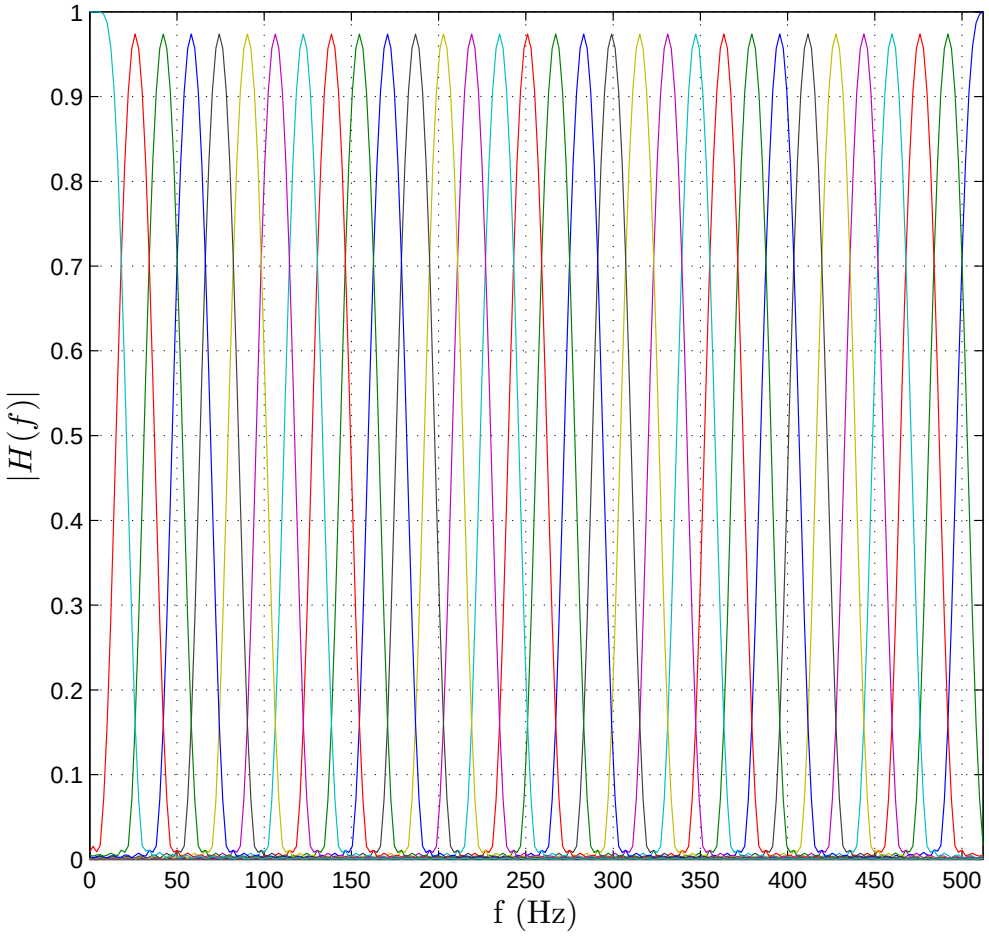

Figure A.1 Frequency response of the analysis filterbank (32 subbands) used in the estimation of the IMF and the IA of a surface EMG signal.

f_filter_bank_ana

Purpose

Compute the subband outputs of the filter bank.

Synopsis

```
[s0, is0]=f_filter_bank_ana(sig,fltana,indfltana)
```

Description

`f_filter_bank_ana` computes the subband coefficients `s0` by convolving the signal `sig` with the filter coefficients `fltana`. Representing the input signal as $x[n]$, for n=$0, 1, 2, 3, \ldots, L-1$ where L is the length of the signal, then we have $x[n]$=`sig`$(n+1)$. The output $y[f, n]$, for f=$0, 1, 2, 3, \ldots, F-1$ and n=$0, 1, 2, 3, \ldots, L+M_f-2$ where F is the number of subbands `n_sb` and M_f is the length of the filter in subband f, is given by $y[f, n]$=`s0`$($`is0`$(f)+n+1)$, for $f > 0$ and `s0`$(n+1)$, for f=0.

Name	Description	Default value
`sig`	column vector of size $L \times 1$ with the coefficients of the input signal	
`fltana`	column vector of size $F\,M_f \times 1$ with the coefficients of the analysis filter bank	
`indfltana`	column vector of size $F \times 1$ with the index of the end of each filter	
`s0`	column vector of size $\sum_{f=0}^{F-1}(L+M_f-1)\times 1$ with the coefficients of each subband	
`is0`	column vector of size $F \times 1$ with the index of the end of each subband	

Example

```
load 'NFF0001_H1_70_EMG'
[sig]=data(:,2);
[fltana, indfltana]=gfb(32);
[s0, is0]=f_filter_bank_ana(sig,fltana,indfltana);
```

See Also

gfb.

tsub

Purpose

Arrange all the computed subband coefficients in a matrix form of size $F \times L$.

Synopsis

```
[tfr]=tsub(s0, is0, shift);
```

Description

`tsub` arranges in a time subband matrix representation all the subband coefficients. This function assumes that all the filters have equal length. The time subband coefficients $y[f,n]$ for f=$0,1,2,3,\ldots,F-1$ and n=$0,1,2,3,\ldots,L+M_f-2$ where F is the number of subbands `n_sb`, L is the length of the signal `sig` and M_f is the length of the filter in subband f is given by $y[f,n]$=`tfr`$(f+1,n+1)$.

Name	Description	Default value
`s0`	column vector of size $\sum_{f=0}^{F-1}(L+M_f-1)\times 1$ with the coefficients of each subband	
`is0`	column vector of size $F \times 1$ with the index of the end of each subband	
`shift`	vector of length two with the number of coefficients to remove from the output `s0` to compensate the increase in the length of the subbands produced by the convolution operation	
`tfr`	time subband matrix representation	

Example

```
load 'NFF0001_H1_70_EMG'
[sig]=data(:,2);
[fltana, indfltana]=gfb(32);
N=length(fltana)/length(indfltana);
shift=[round(N/2),round(N/2)];
[s0, is0]=f_filter_bank_ana(sig,fltana,indfltana);
[tfr]=tsub(s0, is0, shift);
```

See Also

gfb, f_filter_bank_ana.

inst_freq

Purpose

Compute the instantaneous mean frequency of a given signal.

Synopsis

```
[imf]=inst_freq(tfr);
```

Description

`inst_freq` computes the instantaneous mean frequency `imf` from the time subband matrix representation `tfr`. The instantaneous mean frequency $\hat{f}[n]$ at time n=0, 1, 2, 3, ..., $L-1$ is given by $\hat{f}[n]$=`fm`$(n+1)$.

$$\hat{f}[n] = \frac{\sum_{f=0}^{F-1} fy[f,n]}{\sum_{f=0}^{F-1} y[f,n]}$$

Name	Description	Default value
`tfr`	time subband matrix representation of size $F \times L$	
`fm`	column vector of size $L \times 1$ with the instantaneous mean frequency components	

Example

```
load 'NFF0001_H1_70_EMG'
[sig]=data(:,2);
[fltana, indfltana]=gfb(32);
N=length(fltana)/length(indfltana);
shift=[round(N/2),round(N/2)];
[s0, is0]=f_filter_bank_ana(sig,fltana,indfltana);
[tfr]=tsub(s0, is0, shift);
[imf]=inst_freq(tfr);
t=(1:length(sig))/(60*1024); plot(t, imf.*1024);
axis([1 3 0 511]); grid on;
xlabel('Time (min)', 'fontsize', 14, ...
'interpreter', 'latex');
ylabel('Frequency (Hz)', 'fontsize', 14, ...
'interpreter', 'latex');
```

See Also

gfb, f_filter_bank_ana, tsub.

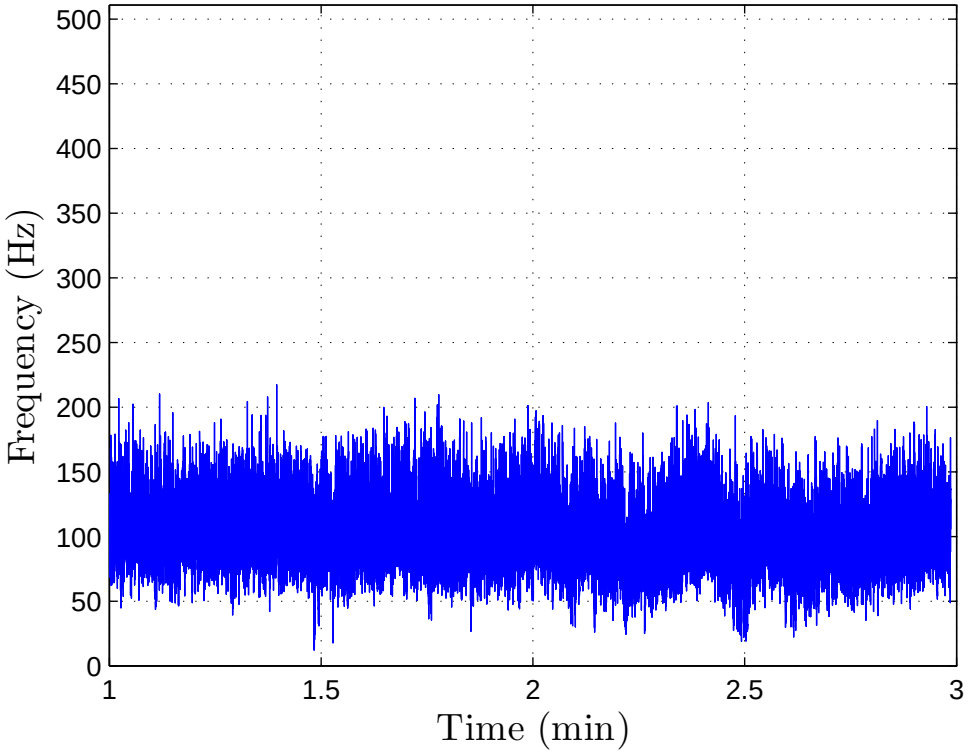

Figure A.2 Instantaneous mean frequency estimated from the input signal `sig` by using 32 channels filter bank.

inst_amp

Purpose

Compute the instantaneous amplitude of a given signal.

Synopsis

```
[i_amp]=inst_amp(tfr);
```

Description

`inst_amp` computes the instantaneous amplitude `i_amp` from the time subband matrix representation `tfr`. The instantaneous amplitude $i_a[n]$ at time n=$0, 1, 2, 3, \ldots, L-1$ is given by $i_a[n]$=`i_amp`$(n+1)$.

Name	Description	Default value
`tfr`	time subband matrix representation of size $F \times L$	
`i_amp`	column vector of size $L \times 1$ with the instantaneous amplitude components	

Example

```
load 'NFF0001_H1_70_EMG'
[sig]=data(:,2);
[fltana, indfltana]=gfb(32);
N=length(fltana)/length(indfltana);
shift=[round(N/2),round(N/2)];
[s0, is0]=f_filter_bank_ana(sig,fltana,indfltana);
[tfr]=tsub(s0, is0, shift);
[i_amp]=inst_amp(tfr);
t=(1:length(sig))/(60*1024);  plot(t, i_amp);
axis([1 3 0 max(i_amp)]); grid on;
xlabel('Time (min)', 'fontsize', 14, ...
'interpreter', 'latex');
ylabel('Amplitude', 'fontsize', 14, ...
'interpreter', 'latex');
```

See Also

gfb, f_filter_bank_ana, tsub.

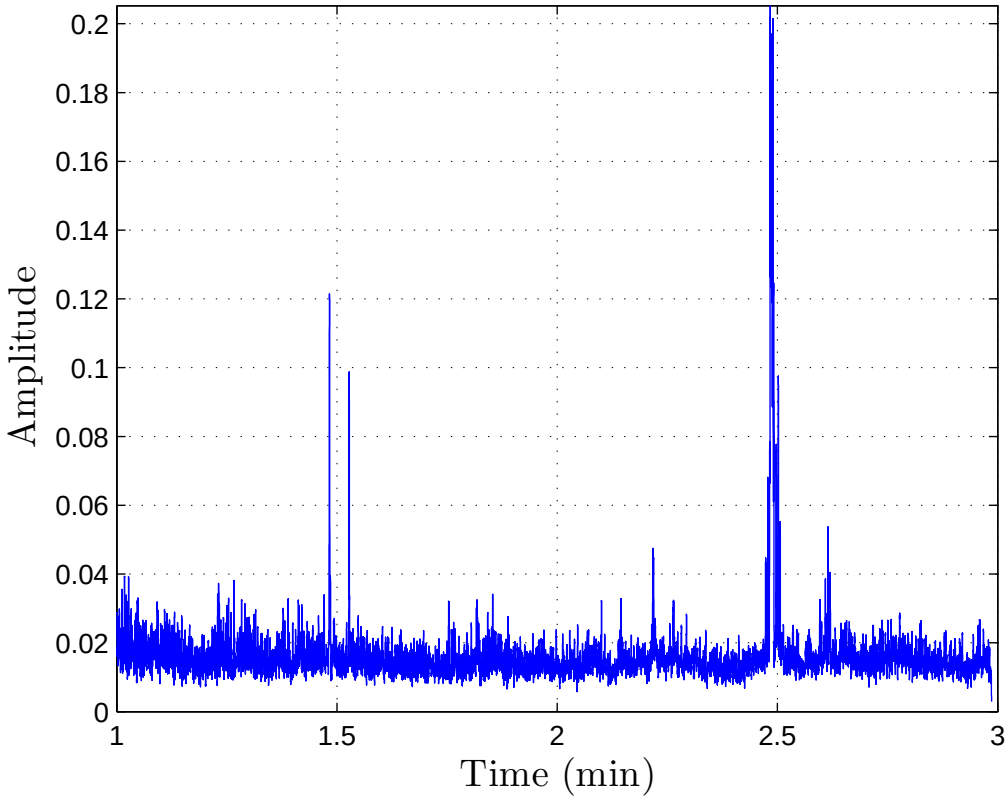

Figure A.3 Instantaneous amplitude estimated from the input signal `sig` by using 32 channels filter bank.

windowing

Purpose

Compute the start and end indices of the location of a rectangular moving window for a specified shift amount.

Synopsis

```
[index_start, index_end]=windowing(nc, L, shift, option)
[index_start, index_end]=windowing(nc, L, shift)
[index_start, index_end]=windowing(nc, L)
```

Description

`windowing` computes the start and end indices of the location of a rectangular moving window for a specified shift amount. This function is useful when we want to apply a rectangular window to a signal of length `L`.

Name	Description	Default value
`nc`	size of the rectangular window, for $1 \leq$ `nc` $\leq$ `L`	
`L`	length of the signal	
`option`	if $\rightarrow 1$ (`index_end` $-$ `index_start`) is always `nc`. The rectangular window is not zero padded at the end of the signal.	1
	if $\rightarrow 0$ (`index_end` $-$ `index_start`) is not always `nc`. The rectangular window is zero padded at the end of the signal.	
`shift`	shifted window, for $1 \leq$ `shift` $\leq$ nc	`nc`
`index_start`	column vector with the start indices	
`index_end`	column vector with the end indices	

Example

```
% Let us suppose that we want to apply a rectangular
% window of 5 points with a shift of  3 to a signal of
% length 15
nc=5; L=15; shift=3;
% when option=1
option=1;
[index_start_1,index_end_1]=windowing(nc, L, shift, option);
% when option=0
option=0;
[index_start_0,index_end_0]=windowing(nc, L, shift, option);

% Output of the code above when option=1
display('index_start_1');

index_start_1 =

     1     4     7    10

display('index_end_1');

index_end_1 =

     5     8    11    14

% Output of the code above when option=0
display('index_start_0');

index_start_0 =

     1     4     7    10    13

display('index_end_0');

index_end_0 =

     5     8    11    14    15
```

fatigue_index

Purpose

Compute a regression-free are ratio index `f_index`.

Synopsis

```
[f_index]=fatigue_index(EMG_variable, K);
```

Description

`fatigue_index` computes a regression-free are ratio index `f_index` from a given surface EMG variable. The surface EMG variable can be either the instantaneous mean frequency or the instantaneous amplitude.

Name	Description	Default value
`EMG_variable`	surface EMG variable	
`K`	size of the window	
`f_index`	column vector with the EMG indices	

Example

```
load 'NFF0001_H1_70_EMG'
[sig]=data(:,2);
[fltana, indfltana]=gfb(32);
N=length(fltana)/length(indfltana);
shift=[round(N/2),round(N/2)];
[s0, is0]=f_filter_bank_ana(sig,fltana,indfltana);
[tfr]=tsub(s0, is0, shift);
[fm]=inst_freq(tsub); K=1024;
[f_index]=fatigue_index(fm, K);
```

See Also

`inst_freq`, `inst_amp`.

B
Questionnaire

Questionnaire to report the perceived levels of discomfort reported by the subject (source — AFRL)

Q1 Have you performed any of the stretching techniques in the last two hours ? (Yes=0, No=6)

Q2 According to the scale, select a number that corresponds to your physical state. (0=No Discomfort, 2=Discomfort, 4=Soreness, 6=Pain)

a Head

b Upper Neck

c Lower Neck

d Shoulders

e Upper Back

f Lower Back

Q3 According to the scale, select a number that corresponds to hot spots or accumulation of perspiration (No Hot Spots, Moderate Hot Spots, Severe Hot Spots).

a Head

b Upper Neck

c Lower Neck

d Shoulders

e Upper Back

f Lower Back

Q4 According to the scale, select a number that corresponds to any numbness or loss of sensation. (0=Normal, 3=Abnormal Sensation, 6=Numbness)

a Head

b Upper Neck

c Lower Neck

d Shoulders

e Upper Back

f Lower Back

Q5 According to the scale, select a number that corresponds to a penetrating ache in your head. (0=No Headache, 3=Minimal Headache, 6=Severe Headache)

Q6 According to the scale, select a number that corresponds to your mental state. (0=Relaxed, 3=Slightly Tense, 6=Restless)

Q7 According to the scale, select a number that corresponds to your mental frame of mind. (0=Alert, 3=Tired, 6=Exhausted)

Q8 According to the scale, select a number that corresponds to your concentration level. (0=Attentive, 3=Distracted, 6=Loss of Focus)

Q9 According to the scale, select a number that corresponds to the effort exerted to perform the MVC at 70%. (0=No Effort, 3=Minimal Effort, 6=Maximal Effort)

C
Matlab Code

```
% function [fltana, indfltana]= gfb(n_sb);
% Purpose:
% Generate the analysis filterbank. For this toolbox the number of subbands
% n_sb can be 16, 32 or 64. We can represent the filter bank in matrix form
% by h[f,n]=fltana(f*Mf+n+1)for f=0,1,2,...F-1 and n=0,1,2,...Mf-1 where F
% is the number of subbands n_sb and Mf is the length of the filter in
% subband f. The length of the filter f can be computed from indfltana
% using Mf=indfltana(f+1)-indfltana(f) for f>0, and indfltana(f+1) for f=0.
% The output indfltana is required only when the filters have different
% length. In this project all the filters used had length equal to 128
% coefficients.
% Synopsis:
% [fltana, indfltana]= gfb(n_sb);
% input vector:
% n_sb:number of subbands
% output vector:
% fltana: column vector with the coefficients of the analysis filter bank
% indfltana: column vector with the index of the end of each filter
% Example:
% fltana, indfltana]=gfb(32);
% hn=reshape(fltana,128,32);
% Hf=fft(hn,512);
% f=linspace(0,511,256);
% plot(f,abs(Hf)); xlabel('f (Hz)','interpreter','latex');
% ylabel('$|H(f)|$','interpreter','latex'); grid on
% #Author: Cristhian Potes
% #Date:   May 23, 2007

function [fltana, indfltana]= gfb(n_sb);
if n_sb==16 | n_sb==32 | n_sb==64
filter{1,1}=['filterbank_' num2str(n_sb) 'subbands'];
load(filter{1,1});
filterbank=filterbank';
[N,M]=size(filterbank);
```

```
fltana=filterbank(:);
indfltana=(N:N:M*N)';
else
disp('Number of subbands has to be 16, 32, or 64');
fltana=[];
indfltana=[];
end
```

```
% function [s0,is0]=f_filter_bank_ana(sig,fltana,indfltana)
% Purpose:
% Compute the subband coefficients s0 by convolving the signal sig with the
% filter coefficients fltana. Representing the input signal as x[n], for
% n=0,1,2,...,L-1 where L is the length of the signal, then we have
% x[n]=sig(n+1). The output y[f,n],for f=0,1,2,...,F-1 and
% n=0,1,2,...,L+Mf-2 where F is the number of subbands n_sb and Mf is the
% length of the filter in subband f is given by y[f,n]=s0(is0(f)+n+1),
% for f>0 and s0(n+1), for f=0.
% Synopsis:
% [s0,is0]=f_filter_bank_ana(sig,fltana,indfltana)
% input vector:
% sig: column vector of size LX1 with the coefficients of the input signal
% fltana: column vector of size F*MfX1 with the coefficients of the
% analysis filter
% bank
% indfltana: column vector of size FX1 with the index of the end of each
% filter
% output vector:
% s0: column vector of size sum(L+Mf-1) for 0<=f<=F+1 with the coefficients
% of each subband
% is0: column vector of size FX1 with the index of the end of each subband
% Example:
% load 'NFF0001_H1_70_EMG'
% [sig]=data(:,2);
% [fltana, indfltana]=gfb(32);
% [s0, is0]=f_filter_bank_ana(sig,fltana,indfltana);
% #Author: Ricardo von Borries, Cristhian Potes
% #Date:   November 13, 2007
function [s0,is0]=f_filter_bank_ana(sig,fltana,indfltana)
sig=sig(:);
down_samp=1;
indsig=length(sig);
indsig=[0;indsig];
```

```
indfltana=[0;indfltana];
lisig=length(indsig);
i0=indsig(lisig-1);
i1=indsig(lisig);
x=sig(i0+1:i1);
sig=sig(1:i0);
indsig=indsig(1:(lisig-1));
lisig=lisig-1;
for i=0:(length(indfltana)-2)
  f=conv(x,fltana((indfltana(i+1)+1):indfltana(i+2)));
  f=f(1:down_samp:length(f));
  sig=[sig;f];
  indsig=[indsig;indsig(lisig)+length(f)];
  lisig=lisig+1;
end
indsig=indsig(2:length(indsig));
is0=indsig;
s0=sig;
```

```
% function [tfr]=tsub(s0, is0, shift);
% Purpose:
% Arrange in a time subband matrix representation all the subband
% coefficients. This function assumes that all the filters have equal
% length. The time subband coefficients y[f,n] for f=0,1,2,...,F-1 and
% n=0,1,2,...,L+Mf-2 where F is the number of subbands n_sb and Mf is the
% length of the filter in subband f is given by y[f,n]=tfr(f+1,n+1.
% Synopsis:
% [tfr]=tsub(s0, is0, shift);
% input vector:
% s0: column vector of size sum(L+Mf-1) for 0<=f<=F+1 with the coefficients
% of each subband
% is0: column vector of size FX1 with the index of the end of each subband
% shift: vector of length two with the number of coefficients to remove
% from the output s0 to compensate the increase in the length of the
% subbands by the convolution operation
% output vector:
% tfr: time subband matrix representation
% Example:
% load 'NFF0001_H1_70_EMG'
% [sig]=data(:,2);
% [fltana, indfltana]=gfb(32);
% N=length(fltana)/length(indfltana);
% shift=[round(N/2),round(N/2)];
% [s0, is0]=f_filter_bank_ana(sig,fltana,indfltana);
% [tfr]=tsub(s0, is0, shift);
% #Author: Cristhian Potes
% #Date:   July 10, 2007

function [tfr]=tsub(s0, is0, shift);
s0=s0(:);
is0=is0(:);
M=length(is0);
L=is0(1);
```

```
tfr=reshape(s0,L,M)';
tfr=tfr.^2;
tfr=tfr(:,shift(1):L-shift); % Compensation of the delay
```

```
% function [fm]=inst_freq(tfr);
% Purpose:
% Compute the instantaneous frequency fm of a given signal from the time
% subband matrix representation tfr. The instantaneous frequency f[n] at
% time n=0,1,2,...,L-1 is given by f[n]=fm(n+1).
% Synopsis:
% [fm]=inst_freq(tfr);
% input vector:
% tfr: time subband matrix representation
% output vector:
% fm: column vector of size LX1 with the instantaneous frequency components
% Example:
% load 'NFF0001_H1_70_EMG'
% [sig]=data(:,2);
% [fltana, indfltana]=gfb(32);
% N=length(fltana)/length(indfltana);
% shift=[round(N/2),round(N/2)];
% [s0, is0]=f_filter_bank_ana(sig,fltana,indfltana);
% [tfr]=tsub(s0, is0, shift);
% [fm]=inst_freq(tsub);
% t=(1:length(sig))/1024; fm=fm*1024; plot(t, fm);
% axis([1 max(t) 0 511]); grid on;
% xlabel('Time[s]', 'interpreter', 'latex');
% ylabel('Frequency[Hz]', 'interpreter', 'latex');
% #Author: Cristhian Potes
% #Date:   Mayo 22, 2007

function [fm]=inst_freq(tfr);
[N,M]=size(tfr);
freqs=(0:N-1)*1/(2*N);
E=sum(tfr);
fm=(freqs*tfr)./E;
fm=fm(:);
```

```
% function [i_amp]=inst_amp(tfr);
% Purpose:
% Compute the instantaneous amplitude i_amp of a given signal from the
% time subband matrix representation tfr. The instantaneous amplitude ia[n]
% at time n=0,1,2,...,L-1 is given by ia[n]=i_amp(n+1).
% Synopsis:
% [i_amp]=inst_amp(tfr);
% input vector:
% tfr: time subband matrix representation of size FXL
% output vector:
% i_amp: column vector of size LX1 with the instantaneous amplitude
% components
% Example:
% load 'NFF0001_H1_70_EMG'
% [sig]=data(:,2);
% [fltana, indfltana]=gfb(32);
% N=length(fltana)/length(indfltana);
% shift=[round(N/2),round(N/2)];
% [s0, is0]=f_filter_bank_ana(sig,fltana,indfltana);
% [tfr]=tsub(s0, is0, shift);
% [i_amp]=inst_amp(tsub);
% t=(1:length(sig))/1024;  plot(t, i_amp);
% axis([1 max(t) 0 max(i_amp)]); grid on;
% xlabel('Time[s]', 'interpreter', 'latex');
% ylabel('Amplitude', 'interpreter', 'latex');
% #Author: Cristhian Potes
% #Date:   Mayo 25, 2007

function [i_amp]=inst_amp(tfr);
ws=1;
ss=1;
[N,M]=size(tfr);
ia=zeros(M,1);
i_amp=ia;
```

```
for i=1:N
    nc=ceil(2*N/ss);
    ss=ss+1;
    [is, ie]=windowing(nc,M,ws,0);
    ana_sig=tfr(i,:);
    for j=1:length(is)
ww=abs(ana_sig(is(j):ie(j)));
ia(is(j))=max(ww);
    end
    ia=ia(:);
    i_amp=i_amp+ia;
    ia=zeros(M,1);
end
i_amp=sqrt(i_amp);
```

```
% function [index_start, index_end]=windowing(nc, L, ,shift, option)
% Purpose:
% Compute the start and end indexes of the location of a rectangular window
% for a specified shift amount. This function is useful when we want to apply
% a rectangular window to a signal of length L
% Synopsis:
% [index_start, index_end]=windowing(nc, L, shift, option); %option default = 1;
% [index_start, index_end]=windowing(nc, L, shift); %shift default =1
% [index_start, index_end]=windowing(nc, L);
% input vector:
% nc: size of the rectangular window, for 1<=nc<=L
% L: length of the signal
% option: if 1 -> (index_end-index_start) is always nc. The rectangular
%   window is not zero padded at the end of the signal
%         if 0 -> (index_end-index_start) is not always nc. The rectangular
%   window is zero padded at the end of the signal
% shift: shifted window, for 1<=shift<=nc;
% output vector:
% index_start: column vector with the start indexes;
% index_end: column vector with the end indexes;
% Example:
% % Let us suppose that we want to apply a rectangular window of 5 points with
% a shift of  3 to a signal of length 15
% nc=5; L=15; shift=3;
% when option=1
% option=1;
% [index_start,index_end]=windowing(nc, L, option, shift)
% when option=0
% option=0;
% [index_start,index_end]=windowing(nc, L, option, shift)
% #Author: Cristhian Potes
% #Date:   Feb 16, 2007

function [index_start, index_end]=windowing(nc, L, shift, option)
```

```
if nargin==3
option=1;
end
if nargin==2
shift=nc;
option=1;
end

if nc>L
disp('Length of the rectangular window nc has to be 1<=nc<=L');
end
if shift>nc | shift==0
disp('Shift of the window has to be 1<=shift<=nc');
end

index_start=1:shift:L;
index_end=nc:shift:L;
dif=abs(length(index_end)-length(index_start));
if dif ~=0
    index_end=[index_end, ones(1, dif).*L];
end
if option ==1
c=find(index_end-index_start+1==nc);
index_start=index_start(c);
index_end=index_end(c);
end
index_start=index_start(:);
index_end=index_end(:);
```

```
% function [f_index]=fatigue_index(EMG_variable, K);
% Purpose:
% Compute a regression-free are ration index f_index from a given surface
% EMG variable. The surface EMG variable can be either the instantaneous
% mean frequency or the instantaneous amplitude.
% Synopsis:
% [f_index]=fatigue_index(EMG_variable, K);
% input vector:
% EMG_variable: surface EMG variable. It can be the instantaneous mean
% frequency or the instantaneous amplitude
% K: Size of the window. It corresponds to the first K samples.
% output vector:
% f_index: column vector with the EMG indices. If the EMG variables has a
% a decreasing pattern then 0<=f_index<=1. If the EMG variable has an
% increasing pattern then f_index<0;
% Example:
% load 'NFF0001_H6_70_EMG'
% [sig]=data(:,4);
% [fltana, indfltana]=gfb(32);
% N=length(fltana)/length(indfltana);
% shift=[round(N/2),round(N/2)];
% [s0, is0]=f_filter_bank_ana(sig,fltana,indfltana);
% [tfr]=tsub(s0, is0, shift);
% [fm]=inst_freq(tsub); K=1024;
% [f_index]=fatigue_index(fm, K);
% #Author: Cristhian Potes
% #Date:   September 10, 2008
% This function is based on Merletti's idea "Indices of Muscle Fatigue".

function [f_index]=fatigue_index(EMG_variable, K)

EMG_variable=EMG_variable(:);
M=length(EMG_variable);
```

```
if K>=2 & K<=M
    EMG_set=EMG_variable(1:K);
    %yr=median(EMG_set);
    yr=EMG_set(1);
    Fk=1 - 1/(yr*(K-1))*(sum(EMG_set(2:length(EMG_set)-1))+...
    EMG_set(1)/2+EMG_set(length(EMG_set))/2);
    f_index(1,1)=Fk;
end

L=2;
    for i=K+1:M
        Fk1=(1-1/(i-1))*Fk + 1/(i-1)*(1-(EMG_variable(i)+...
        EMG_variable(i-1))/(2*yr));
        f_index(L,1)=Fk1;
        L=L+1;
        Fk=Fk1;
    end
```

D
Curriculum Vitae

Cristhian M. Potes

350 North Festival apt 309

El Paso, TX, 79902

(915)3566939

cmpotes@miners.utep.edu

Education

MSc., The University of Texas at El Paso (UTEP)

Doctoral and Master in Electrical and Computer Engineering

Master Expected Graduate: Dec 2008

Doctoral Expected Graduate: Dec 2010

Overall GPA: 3.7/4.0

Relevant Courses

- Computer tomography
- Digital signal processing
- Parameter estimation
- Linear programming
- Random processes
- English technical writing
- Numerical optimization
- Image processing

Honors and Activities

- Texas Instruments Foundation scholarship, Fall 2007, Spring 2008, Fall 2008
- IEEE society, member, 2007-Present
- Maintainer of 10 modules and 1 course of conexions web page http://cnx.org/

Publications

- C. Potes, R. von Borries, C. Jacques Miosso, J. H. Pierluissi. Assesment of Muscle Fatigue from TF Distributions of SEMG Signals. *Twenty-Fourth Southern Biomedical Engineering Conference*, April 2008.
- C. Potes, R. von Borries, C. Jacques Miosso. Wavelet-Based Signal Processing for Monitoring Discomfort and Fatigue. *Air Force Research Laboratory Human Efectiveness Directorate Biosciences and Protection Division Biomechanics Branch*, June 2008.

• R. von Borries, C. Jacques Miosso, C. Potes. Directional Filter Banks for Wavelet Decomposition of Images Based on the Radon Transform. *Forty-First Asilomar Conference on Signals, Systems and Computers*, IEEE Signal Processing Society, November 2007.

• R. von Borries, C. Jacques Miosso, C. Potes. Compressed Sensing Using Prior Information. *The Second International Workshop on Computational Advances in Multi-Sensor Adaptive Processing*, IEEE Signal Processing Society, December 2007.

• C. J. Miosso, R. von Borries, M. Argaez, L. Velazquez, C. Quintero, C. M. Potes. Compressive sensing reconstruction with prior information by iteratively reweighted least-squares. *IEEE Transactions on Signal Processing – correspondences*, July 2008 (under revision).

B.Sc., Universidad Santiago de Cali (USC)

Bachelor in Bioengineering

Graduated: Sept 2006

Overall GPA: 3.9/4.0

Relevant Courses

- Biomedical instrumentation
- Microcontrollers
- Sensors and transducers
- Digital design
- Biophysics
- Electromedicine

Honors and Activities

• Sociedad Colombiana de Ingenieros, Premio Lino de Pombo, 2006

• The best Graduated Student, Honor Graduation, 2006

• Superior Counselor, member, 2003-2006

Experience

UTEP El Paso, TX

Department of Electrical and Computer Engineering Aug 2006 - July 2008

Research Assistant

Project: Wavelet based Signal Processing for monitoring Discomfort and Muscle Fatigue

Advisor: Dr. Ricardo von Borries

Sponsor: Air Force Research Laboratory (AFRL)

Achieved Goals:

• Developed a toolbox in Matlab for the assesment of muscle fatigue

• Processed recorded surface electromyography signals

• Analyzed surface electromyography signals using time-frequency distributions

Universidad Santiago de Cali Cali, Colombia

Department of Engineering Aug 2004 - Jun 2006

Project Engineer

Achieved Goals:

• Managed the repair and maintenance of the biomedical equipment

• Standardized the biomedical equipment

• Implemented the calibration metrology laboratory of biomedical equipment

Technical Skills and Competences

Operating systems: Windows (98, 2000, XP), LINUX/UNIX

Applications: MS Office suite, Electronics Workbench Multisim, Latex, Dreamweaver, Eagle, Labview

Programming languages: C, C++, Visual Basic, Matlab, Assembler, Labview

Excellent problem solving, organization and collaboration skills

Fluent in English and Spanish

Studying Chinese and German languages (Basic Level)

Research Interests

• Time Frequency analysis for non-stationary signals

• Brain Computer Interfaces

• Computerized Tomography

• Neuroengineering

• Wavelets

• Biomedical Image processing